Strategies for Choosing Descent Flight-Path Angles for Small Jets in High-Density Traffic

Minghong G. Wu *

University of California, Santa Cruz, Moffett Field, California, 94035-1000

Steven M. Green†

NASA Ames Research Center, Moffett Field, California, 94035-1000

James Jones ‡

Department of Civil and Environmental Engineering, University of Maryland, College Park, MD 20742

A standard descent procedure with a fixed flight-path-angle (FPA) is proposed to improve trajectory predictability for arriving small jets in the transition airspace into congested terminal area. Three candidate strategies for selecting fuel-efficient and flyable descent FPAs are proposed. The three strategies vary in operational complexity and fuel-burn merits. To mitigate variation of wind among flights, the two simpler strategies are adapted to airport, directions of arrival, and time. Three major US airports with different degrees of wind variation and disparate arrival traffic flows are analyzed. Results show that, when compared to the simple Airport-Static adaptation, the finest adaptation of the simpler strategies recover up to 50%-75% of the extra fuel burn relative to the minimum-fuel strategy. Wind variation, descent altitude restrictions, arrival directions, and fleet composition all affect the fuel efficiency of the simple strategies. Trade-offs between fuel burn and planned speed brake usage in the choice of the FPA are discussed. Fuel efficiency of simple strategies for the entire national airspace in the United States is estimated. Considerations and implications for air navigation service providers are discussed.

*Research Engineer, AIAA Member

†Aerospace Engineer, AIAA Associate Fellow, deceased on 8/31/2013

‡PhD candidate

Nomenclature

ARTCC	Air Route Traffic Control Centers
ATC	Air Traffic Control
BADA	Base of Aircraft Database
CAS	Calibrated airspeed
CDA	Continuous Descent Arrival
CTAS	The Center-TRACON Automation System
DFW	Dallas/Fort Worth International Airport
EDA	Efficient Descent Advisor
FAA	Federal Aviation Administration
FMS	Flight Management Systems
FPA	(Inertial) flight-path angle
JFK	John F. Kennedy International Airport
LAX	Los Angeles International Airport
NAS	National Airspace System
NextGen	Next Generation Air Transportation System
OPD	Optimized Profile Descent
RUC	Rapid Update Cycle
SB0	Speed-Brake-Zero, forbidding speed brake usage
SBANY	Speed-Brake-Any, allowing any degree of speed brake usage
STA	Scheduled time of arrival
TMA	Traffic Management Advisor
TOD	Top of descent
TRACON	Terminal Radar Approach Control
TS	Trajectory Synthesizer
VNAV	Vertical Navigation
γ	Inertial flight-path angle
γ_0	Descent-Speed FPA's baseline descent flight-path angle
γ_{univ}	Universal FPA's descent flight-path angle
f_i	Scaled fuel burn
f_0	Raw fuel burn
N_{R}	Number of RUC weather forecasts
N_i	Number of passenger seats
V_d	Descent CAS issued by the ATC
V_d^0	Lowest descent CAS that can be issued by the ATC without consulting with the pilot

I. Introduction

Trajectory management of metered arrivals into high-density terminal airspace is a critical component of Trajectory-Based Operations, one of the key milestones of the Next Generation Air Transportation System (NextGen).[1–3] Significant research in the past two decades has focused on the utilization of modern flight management systems (FMS) to enable continuous descent planning, at least from cruise to a metering fix at the boundary of the terminal area. Field trials have provided a great deal of insight into the ability to predict and execute such continuous descents for major-carrier type aircraft such as Boeing and Airbus.[4–7] Fuel benefits for continuous descents compared to current-days' operations have also been evaluated.[1,4,8] However, little attention has been paid to "small" (regional, business and light) jet types, which comprise a large and potentially high-growth portion of NextGen traffic operations in the United States.[9]

Predicting the descent profiles of small jets has been challenging. Unlike larger aircraft types, which are equipped with performance-based FMS systems that attempt to optimize the vertical profile with idle or near-idle descents, most small jets are equipped with simple Vertical Navigation (VNAV) capabilities that cannot guide idle-thrust descents. Observations of regional jet operations and pilot interviews revealed that a large variety of descent-planning techniques are used by pilots, even for the same equipment and air carrier. These techniques vary in terms of the selection of descent angle or vertical speed, bottom-of-descent planning, and top-of-descent transition. The intended descent procedure for a specific flight is generally unknown to Air Traffic Control (ATC), and therefore cannot be utilized by ground automation desicion support tools to ensure vertical separation from aircraft at different altitudes. Moreover, the inflexibility of company preferred descent procedures can result in trajectories that are fuel-inefficient or difficult to fly under certain conditions. For example, the "standard operating procedure" of one large regional carrier called for a calibrated airspeed (CAS) of 320 knots for descent, initiated at the cruise Mach number, using a default flight-path-angle (FPA) of -3.8° (negative indicates descent). This works reasonably well for nominal conditions with light to moderate winds and no ATC interruptions to the descent. However, when the winds are strong and speed clearances are issued by controllers for metering and spacing, the nominal descent FPA can become inefficient or difficult, if not sometimes impossible, to fly.

It is desirable to develop a standard descent procedure for arriving small jets in the transition airspace leading to congested terminal areas. This paper proposes a standard fixed-FPA descent procedure that is supported by the simple VNAV of almost all small jets. The selection of an FPA, which is simultaneously known by the pilots and ATC, is expected to realize better trajectory predictability, which in turn would better support Trajectory-Based

Operations and increase airspace throughput. Lack of a descent procedure for small jets can hamper the performance of all trajectory-based ground automation decision support tools for scheduling and spacing. Specifically, a standard descent procedure for small jets was required by the Efficient Descent Advisor (EDA), which was developed to assist en-route controllers achieve fuel-efficient continuous descent arrivals (CDA)[1] that meet the Traffic Management Advisor's[10] (TMA) scheduled times of arrival (STAs) at the metering fix and maintain separation during congested operations.

While a fixed-FPA descent improves trajectory predictability, selecting the FPA is a non-trivial task. The most fuel-efficient and "flyable" FPAs can vary significantly with the winds along the route, wind gradient, descent speed, aircraft type, and aircraft weight.[11] The systematic effect of these variables on the selection of fuel-efficient and flyable FPAs is not well researched, as only limited analysis of fixed-FPA descents exists in the literature.[12–16] Given the significant variation of the winds aloft from one area of the National Airspace System (NAS) of the United States to another, and from one day, week or month to another, the FPA selection may need to be "adaptable."

This paper presents three candidate strategies for selecting descent FPAs for small jets in the transition airspace of a metered environment, where arrival flights are expected to cross the metering fix each at a specific STA. While the three strategies are expected to achieve the same level of trajectory predictability, they vary in operational complexity and fuel efficiency. The minimum-fuel strategy has the best fuel efficiency but highest operational complexity. A methodology was developed to select parameters for the two other simpler strategies and compare their fuel efficiency to the minimum-fuel strategy. Benefits of various adaptations of the two simple strategies to the airport, arrival gate, and periods of time categorized by season, month and day, are estimated. Three major airports of the United States with different levels of wind variation and disparate arrival configurations are analyzed. The analysis reveals how close in fuel efficiency the two simple strategies can get to the minimum-fuel strategy, and helps evaluate which strategy provides the best value for implementation.

The rest of the paper is organized as follows: Section II describes the metered environment and defines the fixed-FPA descent; Section III outlines the three strategies, the methodology for selecting parameters of the strategies, and adaptation of the simple strategies to airspace and time; Section IV analyzes the variation of winds aloft for twelve major US airports and selects three for detailed analysis; Section VI describes the modeling schemes for the metering-constrained arrival trajectories; Section VII presents and compares results of the selected FPAs and relative fuel burn merits between the three strategies for the three airports; Section VII also explores the effect of planned speed brake usage on fuel burn as well as adaptations of the simple strategies to the NAS; Section VIII discusses the implication of the results and considerations for implementation of the simple strategies. Finally, Section IX

summarizes the methodology and the findings.

II. Background

The fixed-FPA descent procedure defines an FPA for the descent profile of a flight in the transition airspace. Consider an arrival flight that is about 150 to 200 nmi away from the destination airport and is transitioning from cruise to descent in 10 to 15 minutes. Figure II depicts a flight that follows a fixed-FPA procedure to descend to the metering fix at the boundary of the terminal area. During periods of congestion, ATC would issue speed clearances to maintain separation and absorb delay. Depending on the difference between the issued descent speed and the metering fix crossing speed, some flights may utilize a short level segment before the metering fix for deceleration. Note that the FPA, γ, the

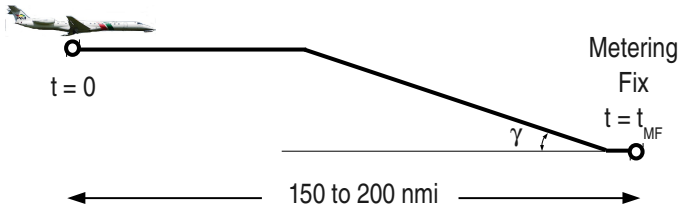

Figure 1. A flight following a fixed-FPA procedure to descend and cross the metering fix at a STA of $t_{\mathbf{MF}}$.

cruise altitude of the arrival flight, and the arrival route define the top-of-descent point in space (ignoring the short level segment before the metering fix). This shared definition is expected to achieve better trajectory predictability by significantly reducing the top-of-descent uncertainty, which has a big impact on the performance of ground-based decision support tools that involve automated separation assurance.[17] This is contrasted with the top-of-descent point for an idle-thrust descent, which is sensitive to the aircraft's performance parameters, aircraft weight, and winds aloft.[18,19] While the fixed-FPA descent procedure is applicable to any level of traffic, it is most beneficial in highly congested traffic scenarios when ATC cannot afford to reserve large airspace buffers to accommodate the uncertainty of the arrival flight's vertical profile. The following discussion and the rest of the paper focuses on the high-density traffic scenario in which arrival traffic is metered and ATC issues speed clearances for all arrival flights.

During periods of congestion in the terminal area, Traffic Management Coordinators in the United States use TMA to plan a schedule that delivers the flights to the runway at a rate that will meet the capacity of the airport. This plan consists of arrival sequences and scheduled times of arrival (STA) at the metering fix, which are typically published points along an aircraft's route of flight and may lie at the boundary of the Terminal Radar

Approach Control (TRACON). TMA computes each flight's STA at the metering fix according to the desired throughput specified by the terminal area control.[10,20] The STA is constantly updated until the arrival flight enters the TMA freeze horizon, where the STA is fixed (frozen) without further adjustment.[20] The definition of a freeze horizon can be time-based or distance-based, and is typically 15-25 minutes or 130-180 nmi away from the metering fix.[20] EDA was developed to assist en-route controllers in achieving TMA's STAs while maintaining separation by computing arrival advisories that also enable fuel-efficient CDA.[1,21–25] During periods of congestion, TMA's STA requires delay with respect to the flight's estimated time of arrival at the metering fix to keep the TRACON arrival traffic manageable.[10] For flights that are about to transition from the cruise phase to the descent phase in a few minutes, EDA utlizes speed reductions in both cruise and descent to absorb up to four minutes of delay.[23] If speed reductions alone are not enough for absorbing the delay, other types of maneuvers such as path stretches are combined with speed reductions.

Early development and simulations of EDA focused primarily on large jets equipped with a performance-based FMS. Later flight tests conducted at Denver Center in the fall of 2010 began to address the descent procedures for small jets. Analysis of 44 fixed-FPA descent trajectories of the Federal Aviation Administration's (FAA) Global 5000 test aircraft showed that errors in the top-of-descent location were 0.5 ± 1.0 nmi.[26] The Global 5000 analysis results suggested that fixed-FPA decents were much more predictable than idle-thrust descents typically performed by large commercial jets, of which the ground predictions had top-of-descent errors around 5 to 10 nmi.[18,27] While a simple, fixed-FPA descent procedure using prescribed clearances was introduced for the purposes of the flight tests, EDA itself lacks a defined descent procedure and corresponding algorithm for small jets. This hampers EDA's capability to deliver small jet arrivals to the metering fix on time and impacts EDA's ability to maintain separation involving the arrival aircraft. A standard descent procedure with proper selection of the descent profile would aid EDA in delivering its full benefits.

Although the analysis in this paper focuses on small jets, the methodology applies to any jet that can fly fixed-FPA descents. In fact, in recent years many Airbus types and new Boeing types have been equiped with VNAV that has fixed-FPA descent guidance.[28]

III. Selection and Definition of the Descent FPA

The criteria for the selection of an FPA consider both fuel efficiency and flyability. A shallow descent may have long and fuel-inefficient descent segments that require excessive thrust. A steep descent may require extensive usage of speed brakes that are operationally unacceptable to pilots. Many pilots are reluctant, if not unwilling, to use speed brakes on a routine basis because of passenger comfort and pilots' desire to reserve the use of speed

brakes for rare occasions. The range of fuel-efficient and flyable FPAs varies with winds, wind gradient, descent speed, and aircraft performance specifics.

The fixed-FPA must be shared between both the pilot and ATC to have benefits of trajectory predictability. Questions arise regarding whether additional infrastructure or equipage would be required for disseminating such information. When considering a selection strategy's potential benefits in fuel and airspace throughput, the complexity of the required changes to the infrastructure and procedures for its implementation should also be considered.

III.A. Three Selection Strategies

Three strategies for defining the descent FPAs are defined below':

- Min-Fuel FPA: computes a flight-specific minimum-fuel FPA
- Universal FPA: selects a universally fixed FPA
- Descent-Speed FPA: defines the FPA as a function of the issued descent speed

While all three are expected to achieve the same level of trajectory predictabilty, they vary in operational complexity and fuel efficiency. Each strategy is further described in the following paragraphs.

The Min-Fuel FPA computes a minimum-fuel FPA to be communicated explicitly to the pilot of each flight just prior to the top of descent (TOD). The computation takes into account the arrival route, weather and wind forecast, aircraft performances, and traffic conditions in real time. Figure 2 sketches the typical fuel burn as a function of the descent FPA for a flight. The Min-Fuel FPA, by definition, selects the minimum-fuel FPA for each arrival flight and

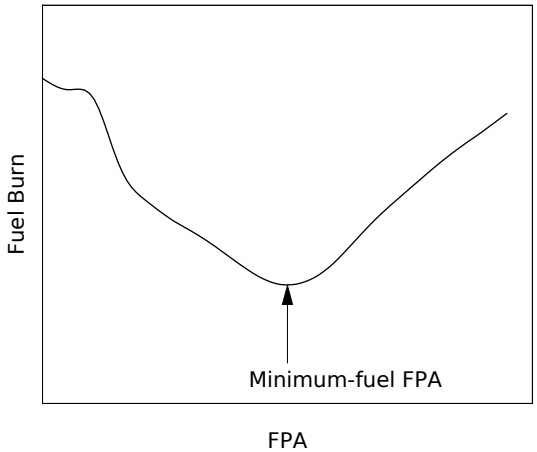

Figure 2. Min-Fuel FPA selects the minimum-fuel FPA.

therefore achieves the best fuel efficiency. However, the requirement of communicating the FPA to the pilot in real time makes it too complex to implement in the near term without datalink. Nonetheless, it serves as a reference point for the fuel burn comparison. The following paragraphs describes two simple strategies that are less fuel efficient but easier to implement.

The Universal FPA defines a single FPA for a large group of flights. This is akin to a glide slope extended from the arrival metering fix back up to the top of descent (TOD) in the en-route airspace. The idea of a universally fixed-FPA descent procedure was explored by Tong et al. at Boeing, with a focus on modifications required for the performance-based FMS equipped jets.[13] The advantage of the Universal FPA is its simple form, which allows it potentially to be published as part of the arrival procedure. The disadvantage is that it does not account for the effects of descent speed, winds aloft along the direction of flight, and other factors, on the range of fuel efficient and flyable FPAs.

The Descent-Speed FPA defines the FPA as a function of ATC-issued descent speed for a large group of flights. This is motivated by the aerodynamical observation that, without considering wind varations, an aircraft flying a slower descent speed on idle thrust would have a shallower descent. The Descent-Speed FPA captures this trend by defining a shallower FPA for a slower descent speed to keep the required power low during descent. The proposed FPA function in this work changes by 0.1° for every 10 knots of descent CAS, a rate observed in a series of test conditions that captures the variation of fuel-efficient FPAs with speed.[11] The FPA function is defined by Equation 1:

$$\gamma = \begin{cases} \gamma_0 & \text{, if } V_d < V_d^0 + 5 \\ \gamma_0 - 0.1 & \text{, if } V_d^0 + 5 \leq V_d < V_d^0 + 15 \\ \gamma_0 - 0.2 & \text{, if } V_d^0 + 15 \leq V_d < V_d^0 + 25 \\ \dots, & \end{cases} \tag{1}$$

where γ is the FPA in degrees, V_d is the descent CAS in knots, V_d^0 is the slowest descent CAS that can be issued by ATC without consulting with the pilots, and the adaptable parameter γ_0 is the prescribed value of γ at V_d^0. V_d^0 is fixed at 250 knots CAS for the analysis in this paper. All values of FPA are negative for the descent, with steeper descents represented by more negative angles. The increment of 0.1° matches the precision of FPA-selection of small jet avionics. Note the selection of the parameter γ_0 defines the entire FPA function. One advantage of the Descent-Speed FPA, like the Universal FPA, is that the function can be determined ahead of time and therefore published as part of the arrival procedure. Moreover, by taking into account the descent speed, the Descent-Speed FPA is expected to be more

fuel-efficient than Universal FPA. The Descent-Speed FPA will not be as fuel-efficient as the Min-Fuel FPA, since it does not account for variation of the winds aloft along the flight direction and other factors on the range of fuel-efficient and flyable FPAs.

III.B. Planned Speed-Brake Usage

In addition to fuel burn, the selection of an FPA should also take into account uncertainties in vertical profile planning. To keep the aircraft on the planned vertical path, power adjustment is preferred to speed-brake deployment for reasons of passenger comfort and the desire of pilots to reserve the use of a speed brake for rare occasions. Besides, some aircraft types have less effective speed brakes than others. Therefore, an upper bound for the planned speed brake usage should be imposed to ensure the flyability of the descent profile.

Two levels of planned-speed-brake usage are considered in this analysis to explore the impact of speed-brake usage on the selection of descent FPA and resulting fuel burn. In one condition, FPAs are limited to those that do not require planned speed-brake usage. This condition , named Speed-Brake-Zero (SB0), is assumed for most of the analysis in this paper. In the other, any FPA is considered valid as long as the estimated amount of speed-brake usage is within the modeled speed brake capacity for that aircraft. This condition, named Speed-Brake-Any (SBANY), is explored for some of the data analysis to understand its effect on the fuel efficiency of strategies.

III.C. Parameters in Universal FPA and Descent-Speed FPA

The FPA of Universal FPA, denoted as γ_{univ}, and γ_0 of Descent-Speed FPA are the parameters that must be selected carefully with consideration for fuel efficiency and flyability. The parameter is sensitive to the prevailing winds aloft and, to a lesser extent, the anticipated traffic demand. The approach in this paper constructs candidate fixed-FPA trajectories from historical flight plans, radar track data, and weather forecasts, and evaluates the aggregated fuel efficiency and flyability as a function of the parameters selected for each strategy. The following criteria are used for selecting γ_{univ} and γ_0:

1. For the parameter considered, at least 99% of the flights must have feasible trajectories, meaning trajectories that have speeds within the performance envelope and satisfy the speed brake usage limits.

2. The parameter should result in the lowest average fuel burn per flight.

The first criterion constrains the steepest γ_{univ} or γ_0 that can be selected, and the second criterion selects the parameter that yields the best fuel efficiency.

III.D. Adaptation of Universal FPA and Descent-Speed FPA

The simplest implementation of the Universal FPA and Descent-Speed FPA would be to apply a static FPA or FPA function to the entire NAS. However, large variation of the environmental conditions such as prevailing winds aloft and local traffic flows impact the fuel efficiency of such procedure, and the magnitude of the impact is not understood. A refined implementation of Universal FPA and Descent-Speed FPA is to adapt their parameters to specific airports. As discussed in Section III.C, the selection of the parameter(s) should be such that the resulting descent FPAs are flyable across significant variations of wind along the route. An airport's arrival traffic configuration also impacts the fuel efficiency of the simple strategies. For airports with opposing arrival directions, particularly the classical four-corner-post configuration, strong winds become problematic. While steeper FPAs are typically more fuel-efficient for arrival flights in a headwind, they can be unflyable for flights in the opposite direction. A shallow FPA would guarantee flyability from both directions, but can be fuel-inefficient for flights in a headwind. These observations motivated the adaptation to the direction of arrival. Compared to a static implementation, adaptation to the direction of arrival achieves a greater degree of customization by mitigating the impact of the variation of winds between flights and thus improves fuel efficiency. While adaptation to the direction of arrival reduces the impact of the variation of along-track winds due to directions, it does not mitigate the impact of the variation of winds over time. The fuel efficiency of the Universal FPA and Descent-Speed FPA strategies can be further improved by adapting to seasonal norms, monthly norms, or even daily predictions.

A set of systematic, temporal and airspace adaptation is presented in Table 1. The columns represent different levels of adaptation for different airspaces, starting with a basic "one-size-fits-all" adaptation for all airports across the NAS. Moving to the right, each

Table 1. Adaptation of Universal FPA and Descent-Speed FPA to time and airspace/direction

Adaptation		Airspace/Direction			
		NAS	Airport	Arrival Gate	Arrival Route
Time	Static				
	Season				
	Month				
	Day				
	Hour				

Min-Fuel FPA

column represents a progressively finer adaptation of the strategies to a specific airport, individual arrival gates (corner posts) feeding an airport, all the way down to specific arrival routes feeding each arrival gate. The rows represent a temporal scale starting at the top with

the simplest option of a static adaptation. Moving down, each row represents a progressively finer adaptation to account for changes in the winds as a function of season, month, day or even hour. The table illustrates the overall approach and potential scope. The Min-Fuel FPA is shown at the bottom-right corner to represent the finest "adaptation" of the simple strategies. The analysis in this paper will assess the adaptation types denoted with white cells in the table. The analysis of adaptations at the level of specific arrival routes and/or hours of the day is left for future work.

IV. Variation of Winds Aloft at Airports

The benefits of adapting the simple FPA selection strategies to airspace/direction and time increases with the variation of winds aloft, the degree of which is different from airport to airport. While some airports may require finer adaptations for the desired level of fuel efficiency, others may achieve reasonable fuel efficiency with a simple Airport-Static adaptation. It is therefore desireable to examine the variations of winds aloft across airports in order to select a set of airports with different degrees of wind variation for application of the FPA selection strategies. In the rest of the paper, reference to winds always refer to the winds aloft, not the winds on the ground.

Twelve major airports of the United States were analyzed for the variation of winds with respect to directions and time of the year. Winds along the route were estimated for four hypothetical arrival routes constructed for each airport. Four hypothetical points in space at four corners around an airport, NE, NW, SE, and SW, were selected at 150 nmi each from the airport and at 35,000 ft in altitude. The vectors connecting each point to the airport defined the four hypothetical routes of arrival. The four points and their routes were used for the estimates of winds along the route. No airport-specific arrival routes were considered here. A year's worth of wind components along the routes of arrival were estimated using the two-hour, 40-km Rapid Update Cycle (RUC) weather forecast[29] for year 2011. The hourly wind forecast amounted to more than 8660 forecast winds.[a] Two quantities, σ_{dir} and σ_{time}, that represented the wind variations with respect to directions and time of the year, respectively, were calculated from the wind components. Let N_{r} denote the number of available RUC wind estimates. The standard deviation of the average wind along each of the four directions, σ_{dir}, is computed by

$$\sigma_{\text{dir}}{}^2 = \frac{1}{4}\sum_{i=1}^{4}(\overline{W_i} - \mu)^2, \text{ where } \mu = \frac{1}{4}\sum_{i=1}^{4}\overline{W_i}. \tag{2}$$

[a]About 1% of the RUC forecast files were not available.

Here $\overline{W_i}$ is the average of the N_r wind components along route i,

$$\overline{W_i} = \frac{1}{N_\mathrm{r}} \sum_{j=1}^{N_\mathrm{r}} W_{i,j}, \tag{3}$$

and $W_{i,j}$ denotes the wind component estimated using RUC wind file j along direction i. The average of the standard deviation of wind for each route, σ_time, is computed by

$$\sigma_\mathrm{time}{}^2 = \frac{1}{4} \sum_{i=1}^{4} \sigma_i{}^2, \text{ where } \sigma_i{}^2 = \frac{1}{N_\mathrm{r}} \sum_{j=1}^{N_\mathrm{r}} (W_{i,j} - \overline{W_i})^2. \tag{4}$$

While σ_dir is indicative of the benefits of adapting the descent FPA to flight directions, σ_time is indicative of the benefits of adapting the descent FPA to time.

Figure 3 shows the estimated wind variations, σ_dir and σ_time, at twelve major airports in the United States. The airports in this figure are ordered from east to west and from

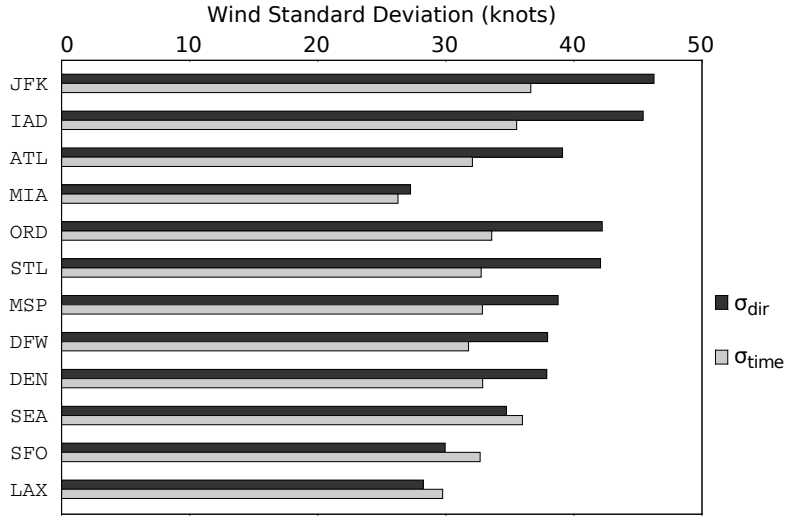

Figure 3. Variation of winds aloft at twelves major airports in the United States for 2011.

north to south. JFK has the highest values of σ_dir and σ_time and hence was chosen as an airport representing large wind variations for the analysis. LAX and MIA have the least wind variations among the twelve airports. LAX was chosen to represent an airport with small wind variations for its large traffic volume and the fact that it is on the West Coast, in constrast to JFK that is on the East Coast. The third airport chosen for the analysis was DFW, which ranks 7th in σ_dir and 9th in σ_time among the twelve airports and represents an airport with medium wind variation. DFW was chosen also for its large volume of small jet traffic and its classical four-corner-post configuration.

Figure 4 contrasts the winds in summer to those in winter at the LAX, DFW, JFK

airports, using the Rapid Update Cycle (RUC) weather forecast in 2011 as an estimate. The wind vectors were computed at 30,000 ft right above the airports, and the coordinates W_E and W_N stand for the east and north components of the wind vector, respectively. Each dot represents a wind vector made by RUC's two-hour forecast, pointing in the direction that the wind is blowing to. Wind vectors from January to March were grouped in the "winter" category, shown in green, while wind vectors from July to September were grouped in the "summer" category, shown in red. Two observations are made regarding the wind distributions at all three airports. Firstly, the winds in winter were stronger, and were predominantly westerly winds. The winds in summer were weaker and more or less isotropic at least for LAX and DFW. Secondly, JFK has stronger winds than DFW, which in turn has stronger winds than LAX. This was consistent with Figure 3 since airports with strong winds are more likely to have strong variations of wind.

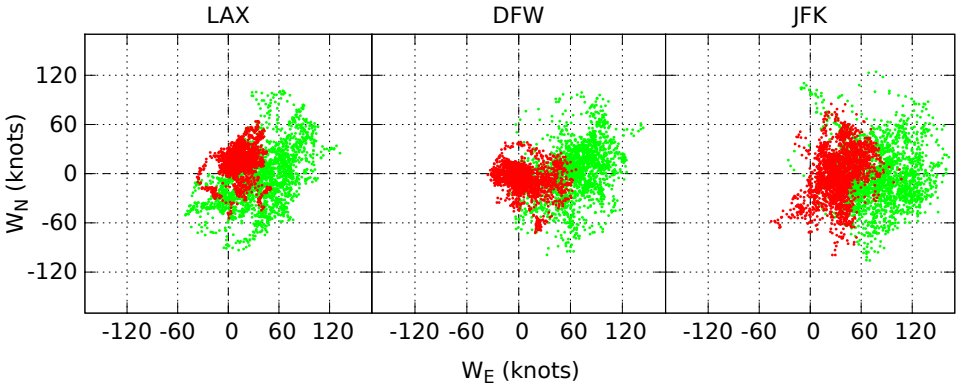

Figure 4. Winds aloft at 30,000 ft in summer and winter of year 2011 at LAX, DFW, and JFK. Red and green dots represent wind vectors in summer and winter, respectively.

V. Small Jet Arrival Traffic for DFW, JFK, and LAX

This section describes the arrival traffic and procedures for small jets in the transition airspace for DFW, JFK, and LAX. DFW is described first because its classical four-corner-post configuration serves as a "textbook" example. Table 2 summarizes the three airports' arrival gates and their associated speed and altitude restrictions. Note that the speed restrictions are defined in CAS. Note that the term "gate" in this paper is used interchangeably with, and has a one-to-one relationship with, the term "metering fix." Therefore, the gate adaptation of the simple strategies should be thought of as an adaptation to a metering fix. This approach ignores the fact that, in actual airspace configuration, a gate can contain more than one metering fix. For example, the east gate for LAX contains both KONZL and GRAMM as metering fixes.

Table 2. The altitude and speed restrictions for arrival flights

Airport	Wind Strength	Gate (Metering Fix)	Altitude (ft)	Speed (CAS in knots)
DFW	Medium	KARLA	11,000	250
		HOWDY	11,000	250
		FEVER	11,000	250
		DEBBB	11,000	250
JFK	Strong	CCC	12,000	250
		CAMRN	12,000	250
		LOLLY	FL200	-
		HARTY	FL210	-
LAX	Weak	KONZL	17,000	280
		GRAMM	FL190	280
		SYMON	12,000	280

V.A. Dallas/Fort Worth International Airport

The Dallas/Fort Worth International Airport has the classical four-corner-post configuration, where an arrival flight enters the TRACON through either of the NE, SE, SW, or NW gate. About two-thirds of its small jet arrivals come from the east. Figure 5 shows radar tracks of arrival flights of small jets on July 28, 2011. The primary metering fixes for the four gates are KARLA, HOWDY, DEBBB, and FEVER. Although there are other fixes for each gate, it was assumed in this analysis that the arrival flights all go through the primary metering fixes. Therefore, the metering fixes KARLA, HOWDY, DEBBB, and FEVER represent the gates. The altitude and speed restrictions at these metering fixes are listed in Table 2. In actual operations, these altitude and speed constraints could depend on a flight's runway assignment and an airport's runway configuration. Such dependencies were not considered in this analysis.

Consider the winds at DFW shown in Figure 4 acting on the arrival flights shown in Figure 5. The prevailing westerly winds in winter resulted in strong headwinds for the eastern gates as well as strong tailwinds for the western gates. In summer, the winds reduced to 60 knots or less most of the time and was somewhat isotropic. Therefore, all four gates experienced similar wind distributions.

V.B. John F. Kennedy International Airport

Figure 6 shows arrival tracks of small jets on January 7, 2011. About 85% of JFK's small jet arrivals were from NW, W, or SW. The remaining arrival flights are from NE. Very

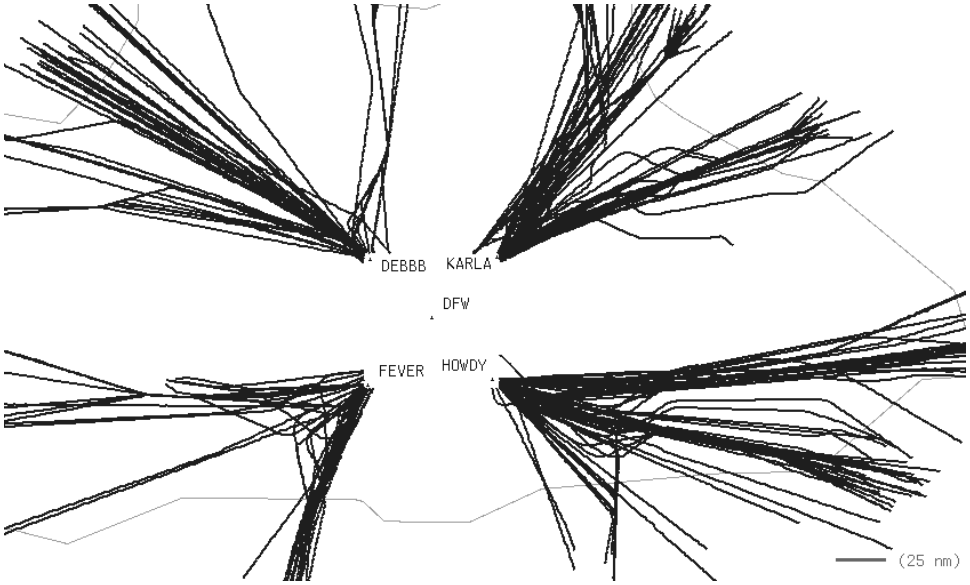

Figure 5. Tracks of arival small jets into DFW on July 28th, 2011.

few small jet flights approached JFK from SE over the Atlantic Ocean. Each arrival jet aircraft entered the TRACON through one of the four metering fixess, characterized by the waypoints CCC, CAMRN, HARTY, and LOLLY, respectively. Two of the four metering fixes

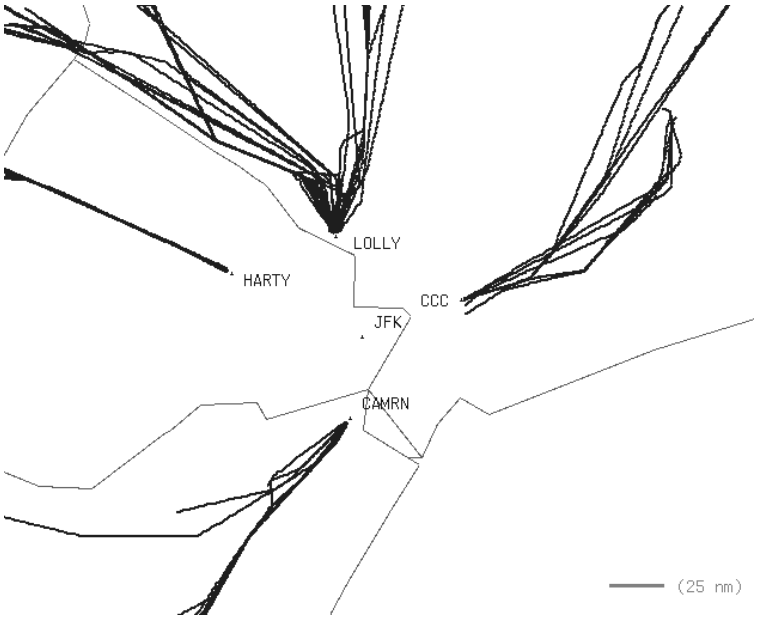

Figure 6. Tracks of arrival small jets to JFK on January 7, 2011.

have restrictions at high altitudes due to the congested airspace in the New York metroplex area. Flights from the N and NW must capture the high-altitude restrictions of FL200 and FL210 ft when they cross LOLLY and HARTY, respectively. Additional downstream altitude and speed restrictions apply, making the vertical profile beyond LOLLY and HARTY very

constrained. For this work, only the portion of the flight trajectory from cruise to one of these four points was considered for varying the FPA. Further desecent segments beyond the first altitude constraints were not considered. This shorter descent segment is expected to diminish the fuel burn differences observed among different values of the descent FPA, and hence diminish the difference in the relative fuel-burn merits of the three selection strategies.

Comparing the wind directions with the arrival directions showed that most flights entering LOLLY, HARTY, and CAMRN, about 80% of the total arrivals, experienced tailwinds. This is in contrast to DFW, in which two-thirds of the flights are from the east and experience mostly headwinds.

V.C. Los Angeles International Airport

Figure 7 shows arrival tracks of small jets to LAX on January 7, 2011. About half of the small jet arrivals were from the NW and the other half from NE and E. Only three arrival metering fixes, characterized by the waypoints GRAMM, KONZL, and SYMON, were found to be utilized by small jets. Note GRAMM and KONZL were treated as different gates in this work although they belong to the same east gate in current days' operation. The altitude and speed restrictions at these three waypoints are summarized in Table 2. Two of the three arrival routes, GRAMM and KONZL, have high altitude constraints at 19,000 ft and 17,000 ft, respectively. Note that GRAMM is part of a newly implemented Optimized Profile Descent (OPD) procedure for LAX.[4] This new procedure actually defines for GRAMM an altitude range, which is between FL210 and 17,000 ft. To keep the altitude restrictions in similar form between gates, the altitude restriction was modeled with a hard value of FL190.

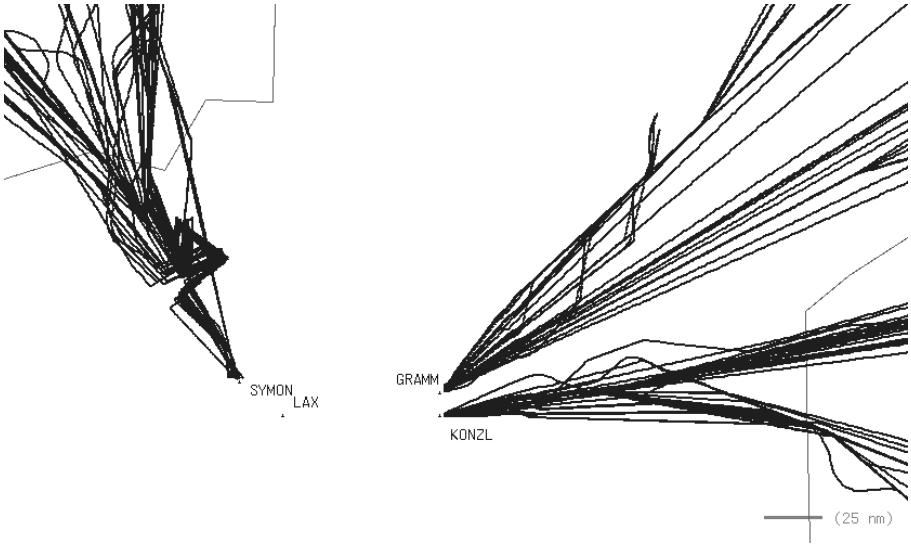

Figure 7. Tracks of arrival small jets to LAX on August 5, 2011.

The magnitude of winds at LAX were smaller than those at DFW and JFK. Flights from the east experienced mild headwinds while flights from the NW experienced mild tailwinds in winter.

VI. Modeling and Analysis Approach

VI.A. Calibrating and Comparing the Three Strategies

Comparison of the simple strategies to Min-Fuel FPA in terms of their fuel merits is a necessary step in a benefit assessment. Other aspects of the comparison of the three strategies include the cost of implementation, which is beyond the scope of this paper. The salient question asked here is: "what FPA strategy would provide the best value for implementation?" To facilitate the fuel-burn comparison, results are presented in terms of the average fuel burn per flight relative to the minimum-fuel solution of Min-Fuel FPA. In this way, the results will show how close the simpler strategies, Universal FPA and Descent-Speed FPA, and their adaptations can come to the minimum-fuel solution without requiring real-time pilot-controller communication of FPA just prior to the top of descent.

A methodology was developed in previous work[11] to compare the fuel benefits of the three strategies of selecting the descent FPA. Conceptually, this methodology consists of two parts: select the parameters for Universal FPA and Descent-Speed FPA; and compare the extra fuel burn of the simple strategies to Min-Fuel FPA for a set of traffic and wind conditions.

The first part of the methodology selects the parameters of Universal FPA and Descent-Speed FPA by analyzing traffic forecast using estimates of winds and temperatures aloft:

- For each arrival flight in the projected traffic demand, evaluate the predicted fuel burn and planned speed-brake usage as a function of the FPA by computing a set of fixed-FPA trajectories.

- Select the value of the parameter based on the aggregated results of speed-brake usage and fuel burn, using the criteria given in Section III.C.

The second part of the methodology estimates and compares the fuel burn of the strategies, using the estimates of winds and temperatures aloft, actual traffic data, and modeled or actual metering delays:

- For each flight, compute the fuel burn and planned speed-brake usage for each flight using all three strategies, which in general select different FPAs. For the Min-Fuel FPA, a set of fixed-FPA trajectories are computed and the FPA with the lowest fuel

burn while satisfying the planned speed brake usage is selected. The extra fuel burn of Universal FPA and Descent-Speed FPA strategies relative to Min-Fuel FPA is recorded.

- Iterate over all flights and compute the aggregated extra fuel burn of Universal FPA and Descent-Speed FPA relative to Min-Fuel FPA.

While the estimates of winds, temperatures aloft, and traffic demand for the second part are, in general, not necessarily the same as that used for the first step, they were the same in the analysis presented in this paper. The RUC data and the radar track data from the Air Route Traffic Control Centers (ARTCC) recorded in 2011 along with a simple metering delay model were used. This means the selection process for the parameters of Universal FPA and Descent-Speed FPA in this analysis used the same wind and track information accessible in real time to Min-Fuel FPA, while in operation the selection process can only be based on forecast or historical data, which may be low-fidelity for longer periods of adaptation time. The fuel benefits of Universal FPA and Descent-Speed FPA obtained in this way should be regarded as an upper bound of the actual benefits.

The implementation of the methodology further simplifies the data collection process by combining its two conceptual parts into one run of a fast-time simulation as described in detail in the following sections. For each arrival flight and a modeled metering delay, the analysis computes a set of trajectories with varying FPA and speed profile that meet the STA. Because the FPA selected by each strategy must be from these trajectories, analysis of these trajectories was sufficient for the fuel burn comparison among the three strategies.

The following sections describe the aircraft modeling, metering delay modeling, meet-time trajectory construction, and data analysis.

VI.B. Route and Vertical Profile

The modeled trajectories considered an arrival flight just entering the freeze horizon towards the transition airspace for metering. A distance-based freeze horizon of 160 nmi was assumed, inside of which TMA would fix the STA for the aircraft.[20] The initial position and speed of the trajectory was picked from a corresponding radar track point. The metering fix that the flight crossed was derived from the track data, and Direct-To trajectories from the initial point to the metering fix were assumed without actually parsing the flight plans for the waypoints.

The vertical profile of an arrival flight was modeled as consisting of up to five segments, as shown in Figure 8. Individual trajectories will contain all or a subset of these segments depending on the speed profile needed to meet the STA. Each segment is modeled by fixing two control parameters. One of the parameters is the FPA; the second depends on the segment. For a cruise segment, the model fixes the airspeed or the engine control for acceleration or

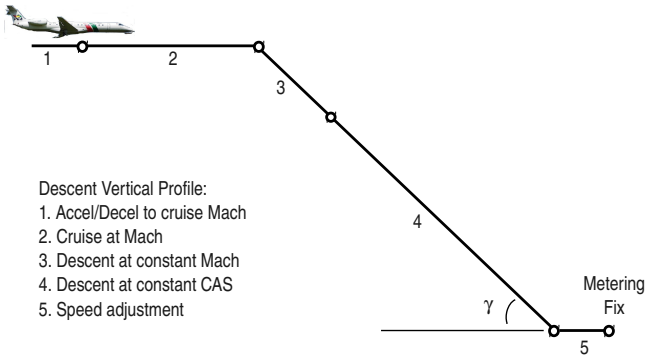

Figure 8. A modeled vertical profile of an arrival flight.

deceleration. For the constant speed descent segments, the model fixes an airspeed in Mach or CAS.

VI.C. Aircraft Modeling

The Trajectory Synthesizer (TS) component[30,31] of the Center-TRACON Automation System (CTAS)[32] was used to compute trajectories and their fuel burn and planned speed-brake usage. While a detailed performance model of small jet types would have been desirable, one was not available. Instead, a high-fidelity CTAS model for a mid-size, narrow-body, twin-jet airliner with a typical descent weight of 170,000 lbs was used. The speed envelopes were selected within the ranges of small jets. Weight uncertainty was modeled by a normal distribution with a 5% deviation of the typical descent weight.

To account for the variation of the fuel-burn rate among aircraft types, the fuel burn was scaled by this empirical formula

$$f_i = f_0 * \frac{N_i + 30}{230}, \tag{5}$$

where f_i is the scaled fuel burn; f_0 is the raw fuel-burn rate calculated by CTAS for the mid-size, narrow-body, twin-engine jet; and N_i is the number of passengers' seats typical of the aircraft type i. This empirical formula was derived by taking the linear regression of the nominal cruise fuel-burn rate of eight small jets plus the mid-sized twin engine jet, using the Base of Aircraft Database (BADA) 3.8 performance model.[33] Although BADA 3.8 provides modeling parameters for small jets, the calibration of these parameters focused on nominal flight conditions only. Since the analysis in this work explored a wide range of the speeds, containing both nominal and off-nominal ones, it was decided that the high-fidelity CTAS model with scaled fuel burn was more appropriate for the fuel-burn analysis.

VI.D. Speed-Brake Usage Modeling

Two levels of planned speed brake usage were considered, Speed-Brake-Zero (SB0) and Speed-Brake-Any (SBANY). SB0 represents the case that FPAs for a flight are limited to those that require no speed-brake usage; SBANY allows any FPA to be considered for a flight as long as the modeled speed-brake usage is within the speed-brake capacity for that aircraft. An empirical constant was used to model the maximum drag coefficient resulting from speed-brake deployment.[11] The results presented in the analysis of the three airports in Section VII assumed the SB0 condition, that is, no planned speed brake usage was allowed in any of the computed trajectories used. The effect of the SBANY on the extra fuel burn of the simple strategies is explored in Section VII.E.

VI.E. Metering Delay

A simple metering delay model was applied to each arrival flight by assigning a random delay time that was independent of the delay times of previous or subsequent flights. The delay at the metering fix was modeled by a uniform distribution between zero and the maximum delay that can be absorbed by speed reductions. No path stretches were considered in this analysis. The delay time was added to the nominal time in order to specify the STA. During the Monte-Carlo simulation (to be described below), two trajectories were computed to define the STA window for random sampling of the delay, using RUC weather forecast and the modeled route described in VI.B. The descent CAS of 320 knots was assumed as the airline-preferred descent CAS and was used together with the aircraft's initial cruise speed in defining the nominal time. The minimum cruise and descent speeds of 220 knots and 250 knots, respectively, were used in defining the slow time. In the absence of a "standard" FPA for defining the nominal trajectory, the two trajectories assumed idle-thrust descent.

VI.F. Fixed-FPA Meet-Time Trajectories

A set of meet-time trajectories with varying FPA and speed profiles was computed for each flight using a modeled metering delay. Here the term "meet-time" refers to the requirement of the trajectories that cross the metering fix at a specific STA. For descent FPAs ranging from -1.8° to -5.5°, with an increment of 0.1°, a meet-time algorithm attempted to compute a fixed-FPA trajectory for each value of the FPA. Fuel burn and planned speed-brake usage was calculated for each meet-time trajectory. These trajectories provided all the fuel-burn data needed for comparison of the three strategies. The algorithm iterated cruise and descent speeds until the trajectory met the desired time-to-fly within a tolerance of 2 seconds. Cruise and descent speeds were related by the Cruise-Equals-Descent speed mode developed for EDA and designed based on operational considerations.[23]

Figure 9 shows a typical range of FPA-descent-speed combinations defining the set of trajectories for a flight meeting an STA. Each square represents the pair of descent CAS and FPA of a trajectory. Trajectories steeper than -3.6° were not shown, because their predicted speed-brake usage exceeded the allowable planned speed brake usage. In most

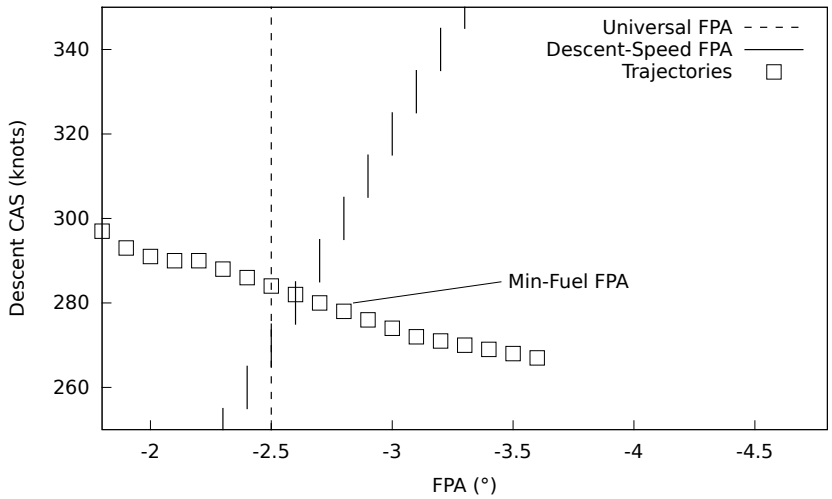

Figure 9. The three strategies select different FPAs in general.

wind conditions, lower descent speeds are required for steeper descent FPAs in order to meet the time. This is because an arrival flight flying a steeper descent FPA would have a longer cruise segment, whose higher ground speed must be compensated for by slowing down in descent.

To illustrate how the descent FPA may be selected differently by the three strategies for the flight, suppose Min-Fuel FPA is used for selecting the FPA. Min-Fuel FPA selects the FPA of the minimum-fuel trajectory, which is found to be -2.8°. Now suppose a set of flights are used for determining the parameters of Universal FPA and Descent-Speed FPA. This set of flights could be on a specific airport or an arrival gate, and during a specific period of time, depending on the type of adaptation. Analysis of this set of flights, determines an γ_{univ} of -2.5° for Universal FPA. A schematic representation of Universal FPA is shown as the dashed vertical line in Figure 9. The resulting meet-time trajectory with the selected γ_{univ} of -2.5 must belong to the set of meet-time trajectories. Therefore, the fuel burn as a result of the selection by Universal FPA for this flight is computed from that trajectory with an FPA of -2.5°. This fuel burn is generally higher than that of the Min-Fuel FPA trajectory with an FPA of -2.8°. Now suppose analysis of the same set of flights determines an γ_0 of -2.3° for Descent-Speed FPA. While the selected FPA must correspond to one of the meet-time trajectories, the relationship between the descent CAS and the FPA of the trajectory must satisfy the FPA function defined in Eq. 1. This FPA function is represented schematically by the solid vertical steps. The fuel burn as a result of the selection by Descent-Speed FPA is

computed from the trajectory that intercepts with the steps representing the FPA function. This trajectory has an FPA of -2.6°. Hence all three strategies select distinct FPAs for this flight.

If no meet-time trajectories have the FPA defined by Universal FPA or satisfy the FPA-descent-CAS relationship defined by Descent-Speed FPA, a failure is recorded for this parameter of the strategy. The number of failures is used to determine whether the parameter is feasible for selection.

VI.G. Simulation and Data Analysis

A fast-time Monte Carlo simulation was performed for each of the airports being analyzed to generate all the meet-time trajectories for small jet arrivals. During the simulation, the metering delay and aircraft weight for each flight were sampled randomly. The fuel burn and speed-brake usage were recorded. All data were categorized by gates and days. Analysis of the meet-time trajectories for all the flights allowed the parameters of Universal FPA and Descent-Speed FPA to be selected. The γ_{univ} for Universal FPA was selected from values between -1.8° and -5.5°, and the γ_0 for Descent-Speed FPA was selected from values between -1.8° and -3.7°. These ranges covered the most fuel efficient values of the parameter under the conditions analyzed. For each γ_{univ} and γ_0, the average fuel burn per flight and feasibility rate were computed for all flights. The feasibility rate was the ratio of the flights with flyable FPAs (total number of success) to the total flights analyzed. It must be 99% or better for γ_{univ} or γ_0 to be selected (see Section III.C). The same selection criteria in Section III.C were used to select γ_{univ} and γ_0 for each of the adaptation types. For the Airport-Static adaptation, all flights arriving at the destination airport were analyzed for the selection. For the gate-specific and Airport-seasonal, -monthly, and -daily adaptations, a subset of the flights arriving at the destination airport was analyzed to select γ_{univ} or γ_0 for a gate and/or a timespan. For example, a total of sixteen pairs of γ_{univ} and γ_0 were selected for the Gate-Season adaptation (four gates times four seasons), each using the flights crossing a specific gate during a specific season. Selection of the parameters based on the feasibility rate ensured that the vast majority of flights would have flyable FPAs, but it did not consider the variation of winds that can make the flights through some gates on some days particularly difficult to fly. To ensure the feasibility rate for any given day and gate was tolerable, a feasibility rate of 80% or better for any pair of gate and day was required for all adaptations. The fuel-burn benefits of trajectories were compared by applying the three strategies. Each trajectory consumed additional fuel with respect to the fuel burn of the minimum-fuel solution of Min-Fuel FPA. By definition, Min-Fuel FPA resulted in zero extra fuel burn. The extra fuel burn for the FPAs selected by Universal FPA and Descent-Speed FPA were computed by aggregating the extra fuel burn from each flight.

A year's worth of the ARTCC track data during 2011 for the three airports, DFW, JFK, and LAX, were used for the analysis. Due to occasional data feed issues, only 95% of the track data were available for the analysis. The flight plan information was used to distinguish the relevant arrival flights from those flying to other airports in the TRACON. Flights that originated in the freeze horizon were not considered. Table 4 lists the number of flights analyzed for each airport and the percentage of flights for each gate.

Table 3. Total number of 2011 flights analyzed for the airports

Airport	Flights	Gate	Percentage (%)
LAX	48692	GRAMM	18
		KONZL	33
		SYMON	49
DFW	81483	KARLA	39
		HOWDY	29
		FEVER	15
		DEBBB	17
JFK	51576	CCC	13
		CAMRN	36
		LOLLY	26
		HARTY	25

Figure 10 shows the ten most frequent small jet aircraft types observed and used for the analysis. The top five most frequent types take up 87%, 93%, and 87% of the entire fleet for LAX, DFW, and JFK, respectively. Note that more large regional jets were observed for JFK (E190 and CRJ9), whereas more small jets such as E135 were observed for DFW.

VII. Results

This section is organized as follows: Sections VII.A, VII.B, and VII.C present the selected FPA and fuel burn comparison for the DFW, JFK, and LAX airports, respectively; Section VII.D compares the fuel burn results between the three airports and identifies the major factors that affect the relative fuel burn merits between adaptation types and strategies; Section VII.E discusses the effect of the speed brake usage condition on the extra fuel burn of the simple strategies; Section VII.F investigates the wind conditions that rendered fuel-efficient shallow descent FPAs; and finally, Section VII.G estimates the fuel efficiency of the two simple strategies adapted to the NAS level, using the analysis result for the three airports.

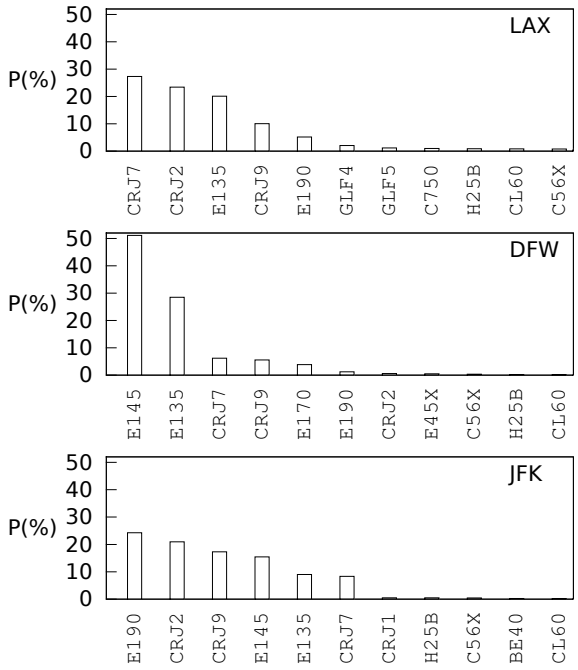

Figure 10. Distribution of types of aircraft analyzed for the three airports.

VII.A. Dallas/Fort Worth International Airport

Section VII.A.1 shows the distribution of FPAs selected by Min-Fuel FPA and discusses their correlation with winds. Sections VII.A.2 and VII.A.3 show the FPA and FPA function selected by Universal FPA and Descent-Speed FPA, respectively. Section VII.A.4 compares the fuel-burn benefits of the three strategies.

VII.A.1. Min-Fuel FPA

Figure 11 presents distributions of the FPAs selected by Min-Fuel FPA categorized by metering fixes. From November to April, steeper FPAs are selected for KARLA and HOWDY whereas shallower FPAs are selected for DEBBB and FEVER. This is expected since DEBBB and FEVER arrivals experienced mostly tailwinds in these months, while flights entering KARLA and HOWDY experienced mostly headwinds. For HOWDY (SE), the third quartile of the selected FPAs reached the steepest -3.5° on Febuary 1, April 15, and April 27. During July and August, the FPAs selected for all four gates were close to -2.6° and -2.7°. This observation was consistent with the weaker winds in summer shown in Figure 4. The direction and magnitude of wind was the strongest discriminator, causing correlated fluctuations of the selected FPAs for all four gates.

Although steeper FPAs are typically selected for strong headwinds, a few exceptions occurred, as shown for KARLA on January 31, Febuary 28, Deccember 21, and December 23, where the first quartile FPA was found to be -1.8°. This suggests that very shallow FPAs

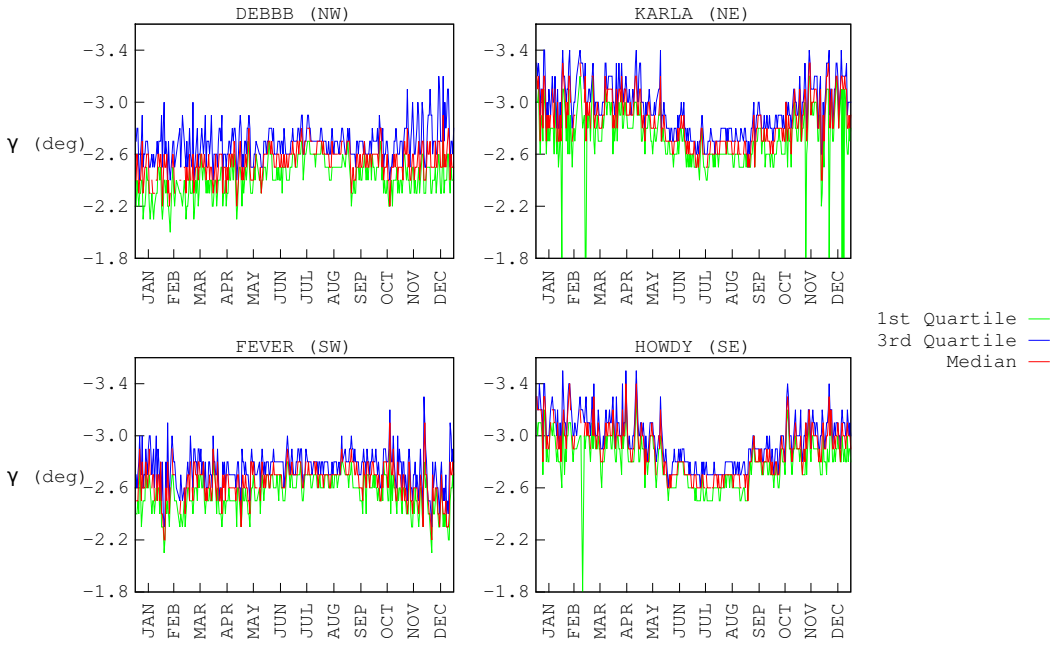

Figure 11. The first quartile, third quartile, and median FPAs selected by Min-Fuel FPA for DFW.

may be the most fuel-efficient in some wind conditions, and will be further investigated in Section VII.F.

VII.A.2. Universal FPA

Figure 12 shows the values of γ_{univ} selected for the airport-specific adaptations of Universal FPA to DFW. In general, the γ_{univ} selected for an adaptation of shorter timespan fluctuated mostly at or above (steeper than) the γ_{univ} selected for a longer timespan. This is because the average of the FPAs of shorter timespan, although possibly fuel-efficient, very often did not satisfy the criteria of the 99% feasibility rate. When the fluctuation of winds is large, the average value may be particularly unflyable on some days and therefore must be rejected. For the γ_{univ} selected for the Airport-Day adaptation, the fluctuation was larger

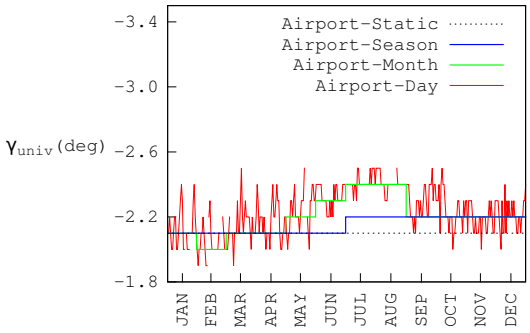

Figure 12. Values of γ_{univ} selected by the airport-specific adaptations of Universal FPA to DFW.

in winter and smaller in summer. The γ_{univ} selected by the Airport-Season adaptation for summer (July, August, and September) appeared to be shallower than most of the Airport-Day values of γ_{univ} during this period of time. This was because the γ_{univ} for this season was bounded by September 5 and 6, which required a shallow FPA of -2.2° for 80% of the flights entering DEBBB to have flyable trajectories.

Figure 13 shows values of γ_{univ} selected for the gate-specific adaptations of Universal FPA. Generally speaking, the selected values of γ_{univ} for KARLA and HOWDY were very close, with HOWDY having slightly steeper values of γ_{univ}. The FPAs for DEBBB and FEVER were very close, with DEBBB having slightly shallower values of γ_{univ}. The variation of Gate-

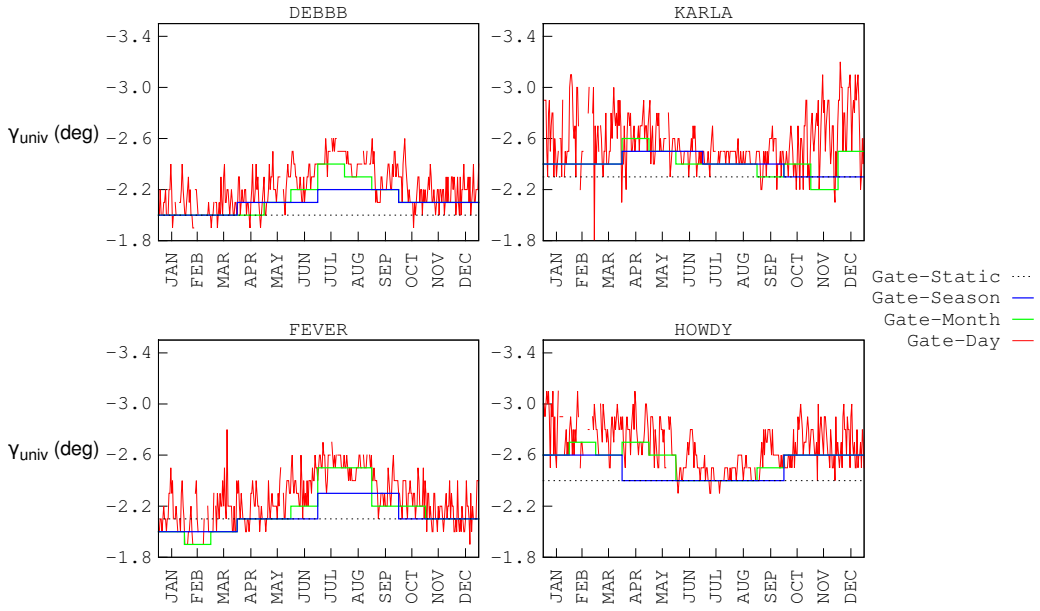

Figure 13. Values of γ_{univ} selected by the gate-specific adaptations of Universal FPA to DFW.

Day γ_{univ} between gates reached 1.2° on April 15, when -3.1° was selected for HOWDY and -1.9° was selected for DEBBB. For a specific gate, the variation of Gate-Day γ_{univ} between days reached 1.4° for KARLA, when -1.8° was selected on February 28 and -3.2° was selected on December 4.

Note that the values of γ_{univ} for the airport-specific adaptations shown in Figure 12 were very close to the values of γ_{univ} selected for DEBBB shown in Figure 13. This is because the selected γ_{univ} must ensure a feasibility rate of 80% for any given gate on any day. Therefore, the γ_{univ} selected for airport-specific adaptations is mostly constrained by the shallowest FPAs selected for DEBBB.

VII.A.3. Descent-Speed FPA

Recall that the family of FPA functions described in Section III.A changes the selected FPA by 0.1° for every 10 knots of the descent CAS. A selected FPA function is defined by the FPA it yields at 250 knots, denoted as γ_0. Figure 14 shows γ_0 selected for the airport-specific

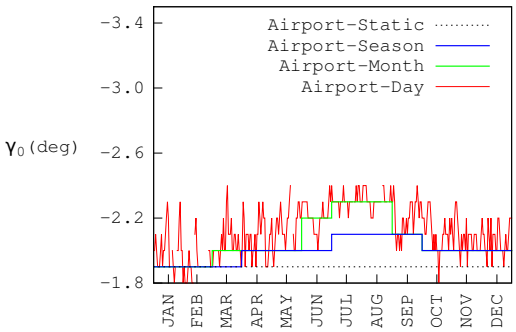

Figure 14. Values of γ_0 selected by the airport-specific adaptations of Descent-Speed FPA to DFW.

adaptations of Descent-Speed FPA. Similar to the values of γ_{univ} in Figure 12, values of γ_0 for an adaptation of shorter timespan fluctuate mostly at or above values of γ_0 selected for a longer timespan. For values of γ_0 selected for the Airport-Day adaptation, the fluctuation is larger in winter and smaller in summer.

Figure 15 shows values of γ_0 selected for the gate specific adaptations of Descent-Speed FPA to DFW. Similar to Universal FPA, γ_0 selected for KARLA on Febuary 28 was -1.8° at

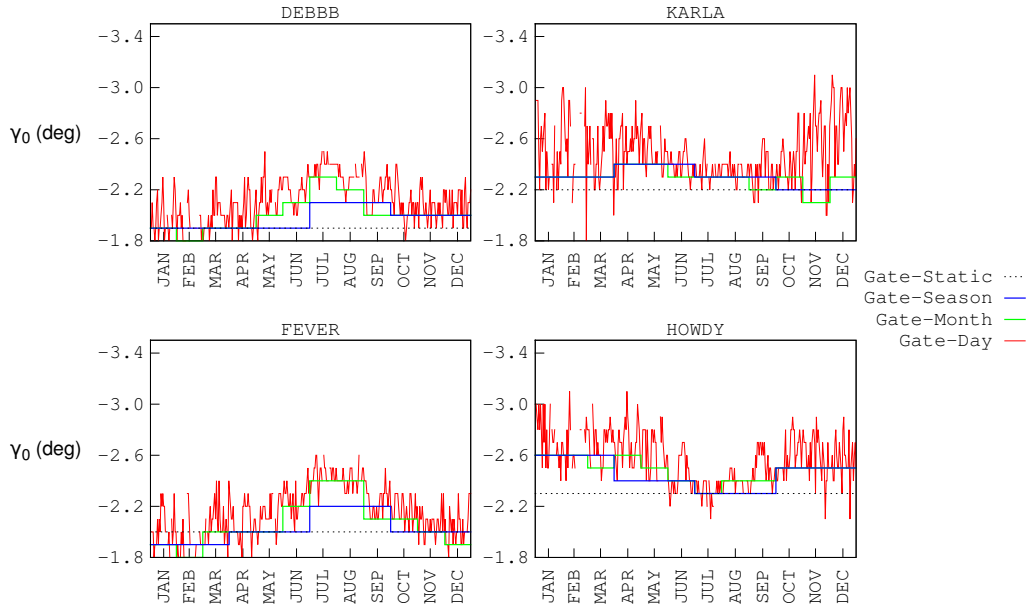

Figure 15. Values of γ_0 selected by the gate-specific adaptations of Descent-Speed FPA to DFW.

250 knots. Similar to Universal FPA, the selection of γ_0 in Figure 14 was constrained by the

results for DEBBB in Figure 15. Therefore the values of γ_0 for airport-specific adaptations were very close to those in the gate-specific adaptations for DEBBB.

VII.A.4. Fuel Burn Comparison

The fuel burn comparison was based on trajectories from the freeze horizon to the metering fix, and therefore had contributions from both the cruise and descent segments. Figure 16 shows the extra fuel-burn per flight computed for Universal FPA and Descent-Speed FPA relative to Min-Fuel FPA. The first observation made was that even the simplest strat-

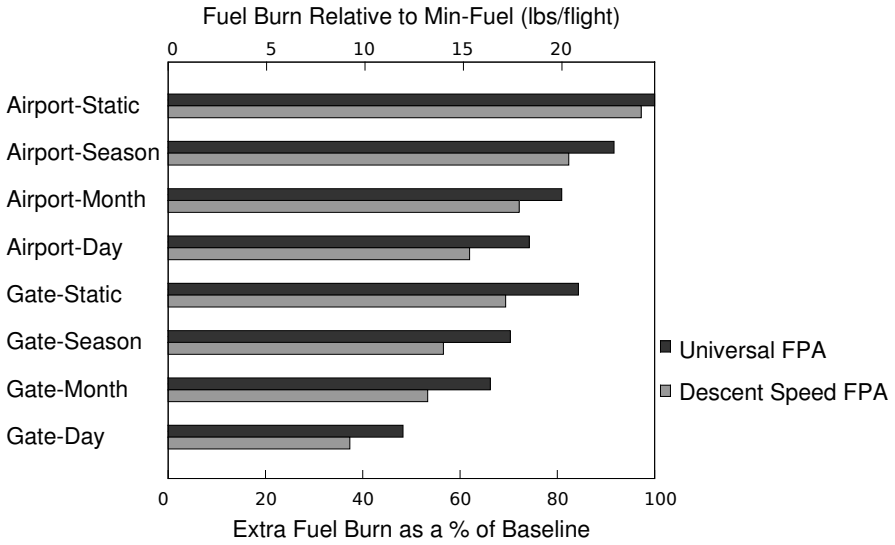

Figure 16. Extra fuel burn calculated for various adaptations of Universal FPAand Descent-Speed FPA to DFW.

egy, a single static FPA adapted for DFW, has the potential to come within 25 lbs of the minimum-fuel solution for each flight on average. To put this into perspective, this represents approximately 5% of the fuel burned by a typical small-jet arrival transitioning over a 160 nmi segment from cruise to the TRACON boundary.

To see the potential impact of directional and temporal adaptations on the fuel efficiency of Universal FPA and Descent-Speed FPA, consider the Universal FPA results first. Relative to the Airport-Static adaptation, the Gate-Static adaptation has the potential to reduce the "extra" 25 lbs of fuel per flight by 16%. In other words, publishing a universal FPA for each of the four gates will recover a little less than a fifth of the way to the minimum fuel solution. By comparison, adapting the universal "airport" FPA to season, month and day has the potential of reducing that extra 25 lbs of fuel per flight by 8%, 19%, and 26%, respectively. When combined, the directional and temporal adaptations together have the potential for reducing the 25 lbs of extra fuel burn by 52%. Essentially, the combined adaptation of a universally fixed FPA for each arrival gate, for each day of operations, recovers more than

half of the fuel savings of the minimum-fuel solution for each flight.

In considering the overall results for Descent-Speed FPA, both the directional and temporal adaptations yield similar improvements in fuel efficiency. By "adapting" to the descent speed, Descent-Speed FPA is essentially a surrogate adaptation for metering delay, one of the primary factors being considered in this analysis. As such, this strategy was anticipated to yield a fair amount of benefit under metering conditions. The results indicate that Descent-Speed FPA contributes a mere 3% reduction in the 25 lbs of extra fuel burn over Universal FPA for the Airport-Static case, and anywhere from 10% to 23% compared to their Universal FPA counterparts. The combined effect of Descent-Speed FPA with both directional and temporal adaptation has the potential to recover 63% of the fuel burn benefits of Min-Fuel FPA.

VII.B. John F. Kennedy International Airport

The selected FPAs for JFK correlated strongly with the winds aloft along the route. The following paragraph discusses the FPAs selected by the gate-specific adaptations of Universal FPA. Results of the other adaptations of Universal FPA and those of Descent-Speed FPA had similar distributions and are shown in the Appendix in Figs A.1, A.2, A.3, and A.4.

Figure 17 shows values of γ_{univ} selected for the gate-specific adaptations of Universal FPA. CCC clearly had the steepest FPAs selected on average compared to the other three gates.

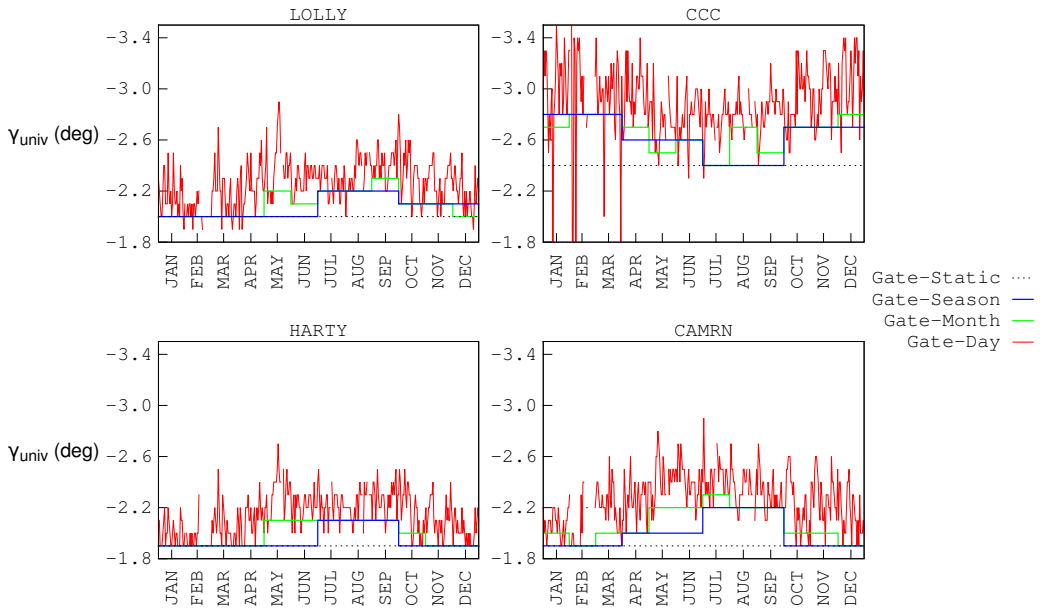

Figure 17. Values of γ_{univ} selected by gate-specific adaptations adaptations of Universal FPA to JFK.

This is in accord with the fact that flights into CCC experienced mostly strong headwinds throughout the year. The other three gates had shallower FPAs selected. The Daily FPAs

selected for HARTY were the shallowest of all gates.

Figure 18 shows the extra fuel burn per flight computed for Universal FPA and Descent-Speed FPA. The Airport-Static adaptation has the potential to come within 22 lbs of the minimum-fuel solution for each flight on average. This amount is slightly less than that

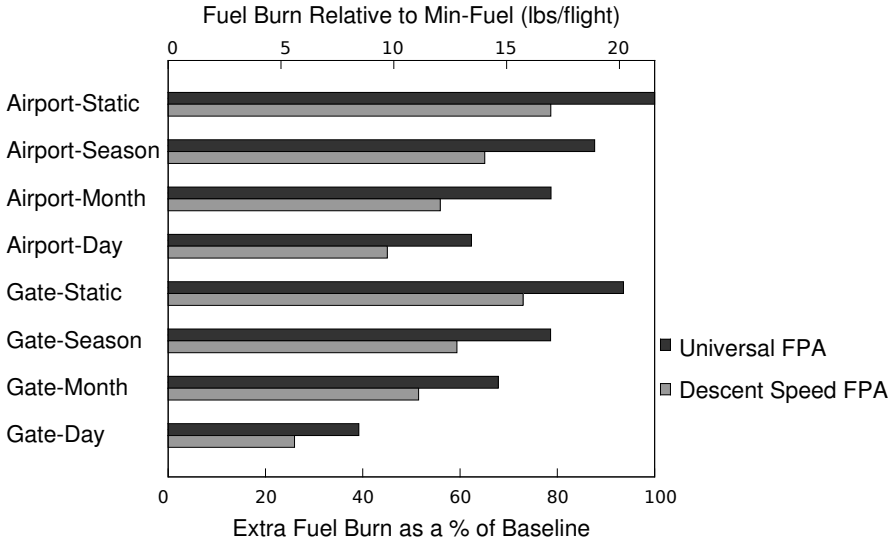

Figure 18. Extra fuel burn calculated for eight adaptations of Universal FPA and Descent-Speed FPA to JFK.

for DFW, and represents approximately 4% of the fuel burn for a typical small-jet arrival transitioning over a 160 nmi segment from cruise to the TRACON boundary. Adapting the universal airport FPA to season, month and day has the potential of reducing that extra 21.5 lbs of fuel per flight by 12%, 21%, and 38%, respectively. Relative to the Airport-Static adaptation, adaptation to the arrival gate only slightly reduces the extra 21.5 lbs of fuel per flight by 6%. Adaptation to gates becomes more effective when combined with finer granularity of timespan, as the Gate-Season, Gate-Month, and Gate-Day adaptations reduce the extra fuel burn from the corresponding airport-specific adaptations by 11%, 14%, and 38%, respectively. The combined adaptation of a universally fixed FPA for each arrival gate, for each day of operations, recovers about 61% of the fuel savings of the minimum-fuel solution for each flight. Descent-Speed FPA contributes a 21% reduction in the 21.5 lbs of extra fuel burn over Universal FPA for the Airport-Static case. In considering the overall results for Descent-Speed FPA, both the directional and temporal adaptations yield similar improvements in fuel efficiency ranging from 22% to 29% among the types of adaptation when compared to Universal FPA counterparts. The combined effect of Descent-Speed FPA with both directional and temporal adaptation has the potential to achieve 74% of the Min-Fuel FPA benefit.

VII.C. Los Angeles International Airport

The magnitude and variation of the winds aloft in LAX was much less than that of DFW and JFK, and the selected FPAs also showed less variation across gates and times. Figure 19 shows values of γ_{univ} selected for the gate-specific adaptations of Universal FPA. The other adaptations of Universal FPA and those of Descent-Speed FPA had similar distributions and are shown in the Appendix in Figs A.1, A.2, A.3, and A.4. One interesting observation is

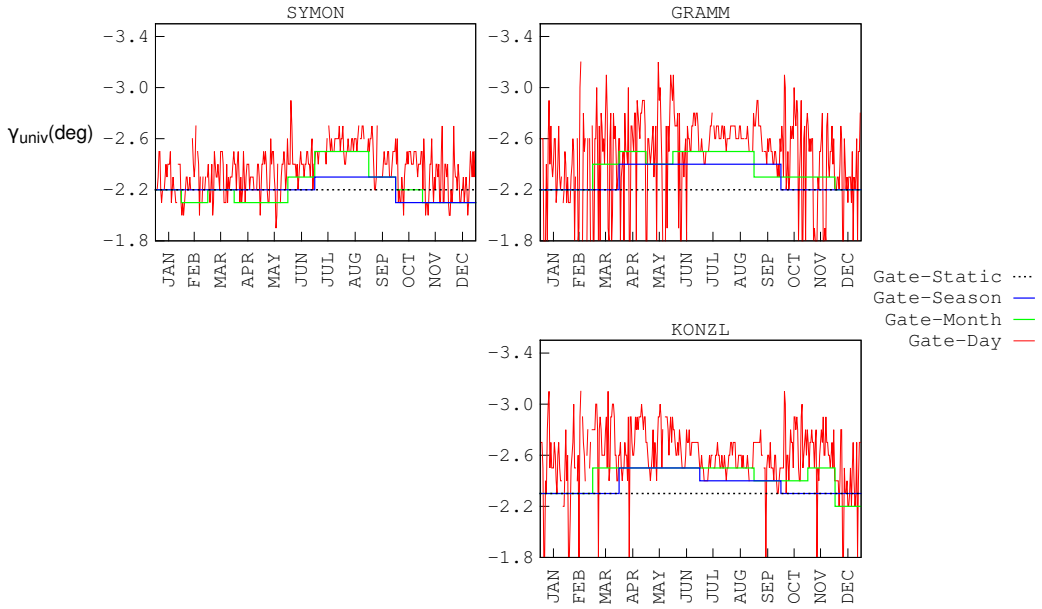

Figure 19. Values of γ_{univ} selected by the gate-specific adaptations of Universal FPA to LAX.

that GRAMM had the shallow FPA of -1.8° selected for many days. This will be further discussed in Section VII.F.

Figure 20 shows the extra fuel burn per flight computed for Universal FPA and Descent-Speed FPA. The simplest strategy, a single static FPA adapted for LAX, comes within 14 lbs of the minimum-fuel solution for each flight on average. Adapting the universal airport FPA to season, month and day has the potential of reducing that extra 14 lbs of fuel per flight by 12%, 21%, and 38%, respectively. Adaptation to the arrival gate is even less effective for LAX than for JFK, only slightly reducing the extra 14 lbs of fuel per flight by 2%. Adaptation to gates becomes more effective when combined with finer granularity of timespan, as the Gate-Season, Gate-Month, and Gate-Day adaptations reduce the extra fuel burn from the corresponding airport-specific adaptations by 5%, 17%, and 34%, respectively. The combined adaptation of a universally fixed FPA for each arrival gate, for each day of operations, recovers about 44% of the fuel savings of the minimum-fuel solution for each flight.

Interestingly, Descent-Speed FPA with Airport-Static adaptation performs slightly worse

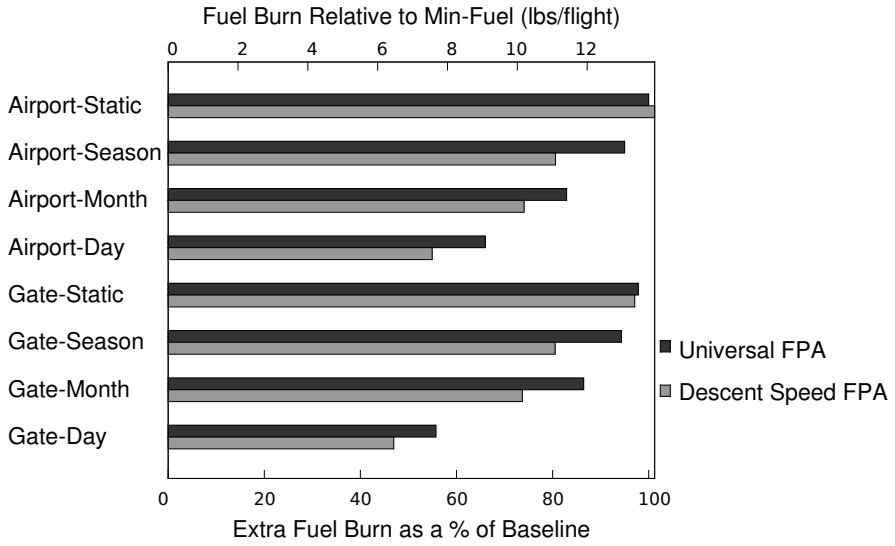

Figure 20. Extra fuel burn calculated for eight adaptations of Universal FPA and Descent-Speed FPA to LAX.

than the Universal FPA's counterpart by 1%. Other directional and temporal adaptations of Descent-Speed FPA do yield mild improvements in fuel efficiency ranging from 1% to 17% among the types of adaptation when compared to Universal FPA counterparts. The combined effect of Descent-Speed FPA with both directional and temporal adaptation has the potential to achieve 53% of the Min-Fuel FPA benefit.

VII.D. Comparison of the Three Airports

This section compares results of the analysis for the DFW, JFK, and LAX airports in terms of the selected FPAs and fuel burn merits of the simple selection strategies. Such comparison gives insight to the design of a fixed-FPA descent procedure by identifiying a set of leading factors that can potentially affect the decision.

The FPA selected by the Airport-Static adaptation of the Universal FPA showed correlation with the variation of winds aloft. Recall that LAX had the mildest variation of winds while JFK had the strongest variation of winds of all three airports. Table 4 shows that, going from top to bottom, shallower FPAs were selected for airports with stronger variation of winds. The extra fuel burn for the Airport-Static adaptation, however, does not show a clear trend. This is mainly due to the fact that the extra fuel burn for LAX and JFK was reduced by the shorter descent segments analyzed for gates that have high-altitude restrictions. A trend would have been seen for the extra fuel burn if the altitude restrictions were similar among the airports.

Compared to the Airport-Static adaptation, the Gate-Static adaptation had the most benefits when the gates were dissimilar in terms of the winds along the route. This was the case for DFW, when the Gate-Static adaptation of Universal FPA recovered 16% of the extra

Table 4. FPA and extra fuel burn for the Airport-Static and Gate-Static adaptation of Universal FPA

Airport	FPA Airport-Static	Extra Fuel Burn (lbs) Airport-Static	Extra Fuel Burn (lbs) Gate-Static	% Fuel Recovered
LAX	-2.2°	13.8	13.5	2%
DFW	-2.1°	24.7	20.8	16%
JFK	-1.9°	21.6	20.2	6%

fuel burn of the Airport-Static adaptation. This is in contrast to JFK and LAX, for which the Gate-Static adaptation only recovered 6% and 2%, respectively. DFW's four-corner-post arrival configuration had two tailwind prevailing gates and two headwind prevailing gates. JFK had three tailwind prevailing gates that account for more than 80% of the small jet arrival traffic. LAX had small wind variations for all three gates. Therefore, the benefits of the Gate-Static adaptation relative to Airport-Static was much smaller for JFK and LAX.

Figure 21 shows the FPA selected for each gate by the Gate-Static adaptation of Universal FPA. The gates are grouped by airports in the order of LAX, DFW, and JFK from top to bottom. These values were also shown as dotted lines in Figures 13, 17, and 19. It is clear

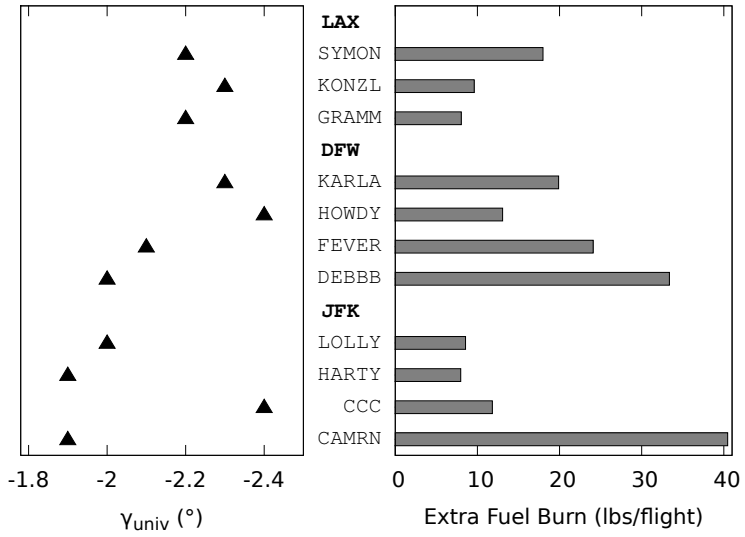

Figure 21. Universal FPA: Gate-Static: The $\gamma_{\mathbf{univ}}$ and extra fuel burn for each gate.

that, as the variation of winds aloft increases, selected FPAs separate into "tailwind" and "headwind" groups. For LAX, the FPAs selected for the three gates SYMON, KONZL, and GRAMM, were close to one another and differ by only -0.1°. For DFW, shallower FPAs were selected for the tailwind-prevailing gates of FEVER and DEBBB, whereas steeper FPAs were selected for the two headwind-prevailing gates of KARLA and HOWDY. The two sets of FPAs are separated by at -0.2°. For JFK, an FPA of -2.4 was selected for

the headwind-prevailing gate, CCC, while shallower FPAs were selected for the other three tailwind-prevailing gates. The three shallower FPAs were different than the other FPA by -0.4°.

Figure 21 also shows the extra fuel burn of the Gate-Static adaptation, associated with each gate, on the right side of the figure. Note that these values were not shown in Figures 16, 18, and 20, whose extra fuel burn for the Gate-Static were aggregated over all gates in each airport. In addition to the variation of winds with time, which increases the extra fuel burn, three other major factors impact the extra fuel burn of a Gate-Static adaptation:

- The direction of wind along the route impacts the extra fuel burn in an interesting way. It was observed that many headwind distributions diminished the fuel burn difference among trajectories with varying FPAs. The fuel burn becomes a weak function of the FPA, and sometimes a very shallow FPA burns less fuel (to be discussed in Section VII.F). As a result, headwind-prevailing gates tended to have less extra fuel burn than tailwind-prevailing gates. KARLA and HOWDY had less extra fuel burn than FEVER and DEBBB mainly because the former two gates are headwind-prevailing.

- High-altitude constraints reduce the length of the descent segment and diminish the difference between trajectories. As a result, the fuel burn difference between different FPAs is reduced. The gates of GRAMM and KONZL for LAX and LOLLY and HARTY for JFK had high-altitude constraints, and therefore the extra fuel burn for these gates were much reduced.

- The aircraft fleet composition directly impacts the absolute values of the extra fuel burn. JFK has larger regional jets and therefore its gates can potentially have more extra fuel burn than LAX and DFW.

Comparison of the extra fuel burn of Descent-Speed FPA to those of Universal FPA showed that, across the airport-specific and gate-specific adaptation types, Descent-Speed FPA was more effective for JFK and DFW than for LAX. A closer look reveals that Descent-Speed FPA was more beneficial for tailwind-prevailing gates than head-wind prevailing gates. Figure 22 shows the γ_0 for each gate by the Gate-Static adaptation of Descent-Speed FPA. Compared to Universal FPA, Descent-Speed FPA reduced the extra fuel of gates prevailed by strong tailwinds, such as CAMRN, DEBBB, and FEVER, by 27%, 24%, and 23%, respectively. Descent-Speed FPA did not reduce the extra fuel of the other gates more than 15%.

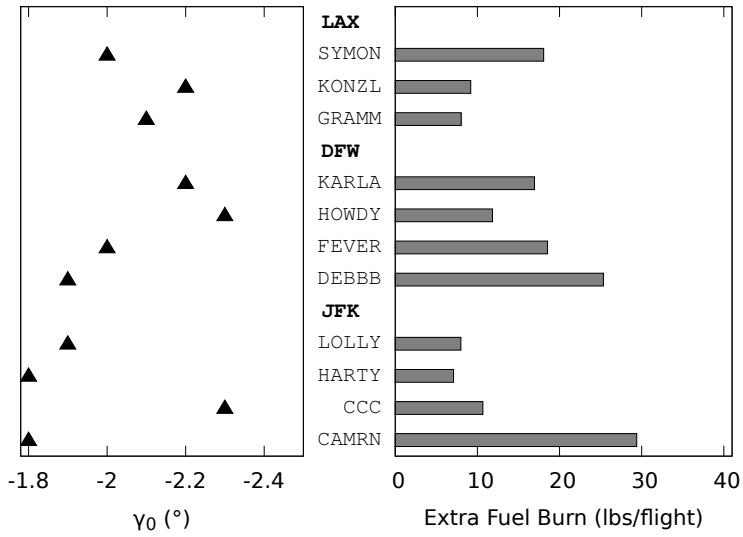

Figure 22. Descent-Speed FPA: Gate-Static: The γ_0 and extra fuel burn for each gate.

VII.E. Effect of Speed-Brake Usage on Fuel Burn

Recall that two levels of planned speed-brake usage, SB0 and SBANY, were described in Section III.B. The SB0 condition ensured that planned-speed brake usage was not required; i.e., the aircraft always maintained a clean configuration during descent. This restriction had an effect on the selected FPA and the resulting extra fuel burn when compared with the SBANY condition. Figure 23 shows the extra fuel burn computed for the Airport and Gate adaptations of Universal FPA applied to DFW, using the SBANY condition. The results with the SB0 condition are shown for comparison. The SBANY condition reduced the extra

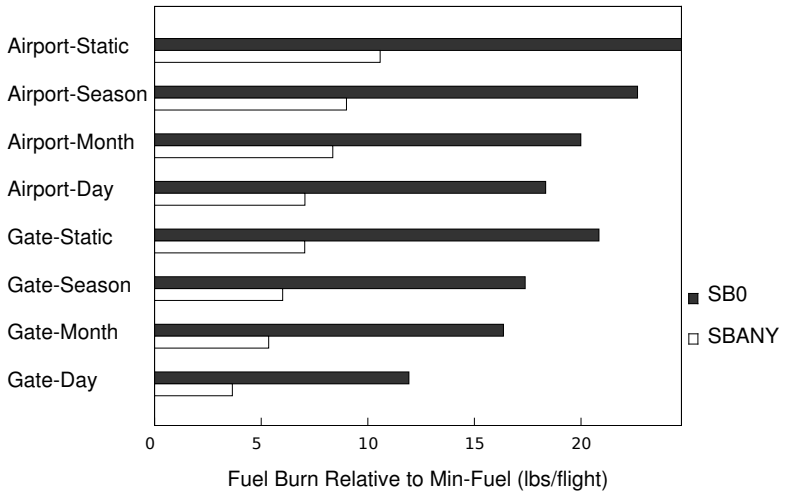

Figure 23. Impact of different levels of the planned speed brake usage on the extra fuel burn, when applied to DFW.

fuel burn of each adaptation type of the SB0 condition by 55% to 70%.

Figure 24 shows the sizable effect that the planned-speed-brake usage had on the feasibility rate and, therefore, the selection of the parameters and the fuel burn for a group of flights. This figure sketches a notional average fuel burn per flight and feasibility rate as a function of γ_{univ} or γ_0. The γ_{univ} or γ_0 that yields the least average fuel burn per flight while having a feasibility rate of at least 99% was selected. The SB0 condition ensured that

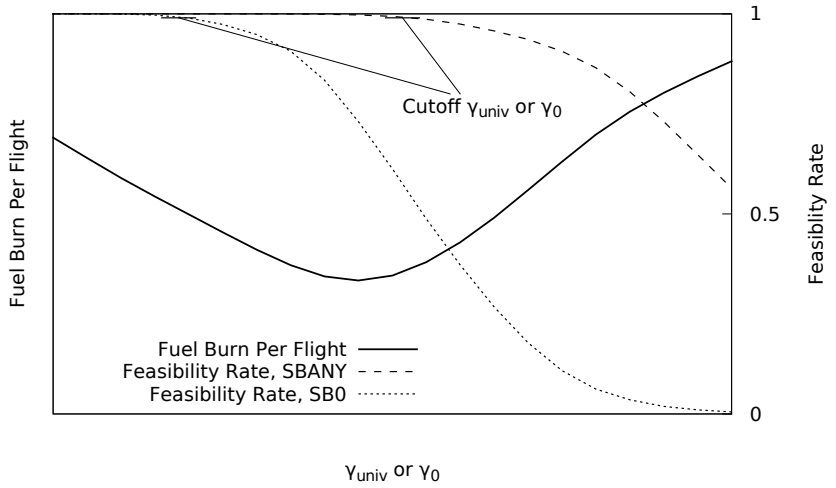

Figure 24. Notional representation of the average fuel burn and feasibility rate. The feasibility rate falls off at steeper values of γ_{univ} or γ_0.

planned speed brake usage was not required, which resulted in an early fall-off of the feasibility rate and therefore a steeper cutoff FPA that would restrict the acceptable γ_{univ} or γ_0 to shallower values. The more forgiving SBANY condition very often allows the minimum-fuel FPA (aggregated over flights) to be selected, as the computed cutoff γ_{univ} or γ_0 (using the criterion of 99% feasibility rate) for SBANY is frequently steeper than the minimum-fuel γ_{univ} or γ_0.

The significant difference between the extra fuel burn of SB0 and SBANY suggested that, in actual operations, it may be worthwhile to trade the robustness of SB0 for the fuel efficiency of SBANY by a planned speed brake usage that allows certain fraction of the speed brake to be deployed. A way of quantifying the concept of robustness would be needed for such a analysis.

VII.F. Fuel-Efficient Shallow Descents

Analysis of the fixed-FPA arrival trajectories showed that headwinds shift the minimum-fuel FPA to a steeper value whereas tailwinds shift the minimum-fuel FPA to a shallower value. Some headwinds, however, also tend to reduce the fuel burn for shallow FPAs. In these wind conditions, the shallowest FPA analyzed, -1.8°, can turn out to be the minimum-

fuel FPA. Figure 25 demonstrates the fuel burn as a function of the FPA for two E145 flights from 160 nmi away to the NE gate KARLA at DFW. EGF2708 arrived at DFW on Feburay

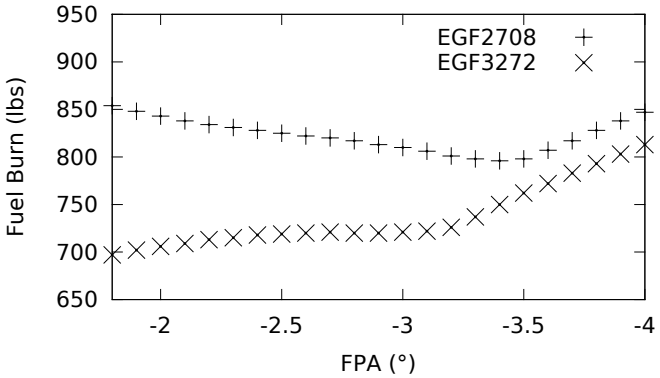

Figure 25. Fuel burn as a function of the FPA for two flights. While EGF2708 had a minimum-fuel FPA of -3.4°, EGF3272 had a minimum-fuel FPA of -1.8°.

1 and had a minimum-fuel FPA at -3.4°. Such minimum-fuel FPA in the middle of the range of sampled FPAs is characteristic of the meet-time trajectories of most arrival flights. EGF3272 arrived at DFW on Febuary 28 and the fuel burn had an inversion in slope that resulted in -1.8° (the shallowest FPA analyzed) being the minimum-fuel FPA. The Gate-Day adaptation of Universal FPA could have selected -1.8° if a majority of the arriving flights had this inversion.

Analysis of the winds aloft along the route revealed that such inversion of slope was highly correlated with the wind gradient with respect to the altitude. Instead of fighting against a strong headwind at a high altitude, if may be advantageous for the aircraft to descend early down to altitudes with a weaker headwind or even a tailwind. Take the two flights in Figure 25 as an example. Between FL360 and FL250 during the descent, the headwind experienced by EGF2708 decreased from 110 knots to 90 knots, while the headwind experienced by EGF3272 decreased from 120 knots to 60 knots. The faster decay of the headwind for EGF3272 contributed to favoring an early descent. Equation 6 considers an average wind gradient experienced by a flight:

$$W' = \frac{(W(x, y, z, t, \Psi) - W(x, y, z - \Delta z, t, \Psi))}{\Delta z}, \tag{6}$$

where W' represents a measure of the change of the wind along the route with respect to altitude, x, y, z, t represent the flight's initial 4D position for the analysis, Ψ represents the flight's heading, and Δz represents a characteristic change of altitude. A value of 8,000 ft was chosen for Δz. Calculation of W' for all flights arrving at DFW through KARLA showed that, on average, the flights on Feburay 28 experienced the greatest change of the along-the-route wind. The average value of W' for the flights entering KARLA was 4.4 knots per

1,000 ft. This was correlated with the shallow FPA selected for Febuary 28 as shown in Figure 13. Interestingly, the Gate-Day adaptation for GRAMM of LAX also selected -1.8° on many days of the year, despite the smaller wind magnitudes in LAX. Analysis of the wind gradient at LAX revealed that the average value of W' also correlated strongly with the occurrence of the selected shallow FPA. Nonetheless, the correlation is not 100%, and other factors such as descent altitude ranges affect the fuel burn as well.

In actual operations, a shallow FPA may extend the descent phase beyond the center boundary or cause more sector crossings, and implementation and execution of such shallow descents can be problematic. Therefore, airspace-related constraints must be taken into account when selecting the FPA for the simple strategies.

VII.G. Adaptation to the NAS

To demonstrate the applicability of the methodology presented in this paper, analysis results of Universal FPA for the three airports of DFW, JFK, and LAX, were aggregated and used to select the FPA for the NAS adaptation types. While the three airports already covered a wide range of wind variation and disparate arrival traffic flows, additional analysis for other airports can be easily incorporated to improve the fuel burn estimates for the NAS adaptation types. Note that the aggregation averaged fuel burn over all the flights analyzed in the three airports, with each flight given the same weight.

Figure 26 showed that the NAS-Static adaptation of Universal FPA resulted in an extra fuel burn of about 27 lbs per flight. As the adaptation moves towards finer granularity of timespans, airspace, and direction, the extra fuel burn reduces. Interestingly, the NAS-

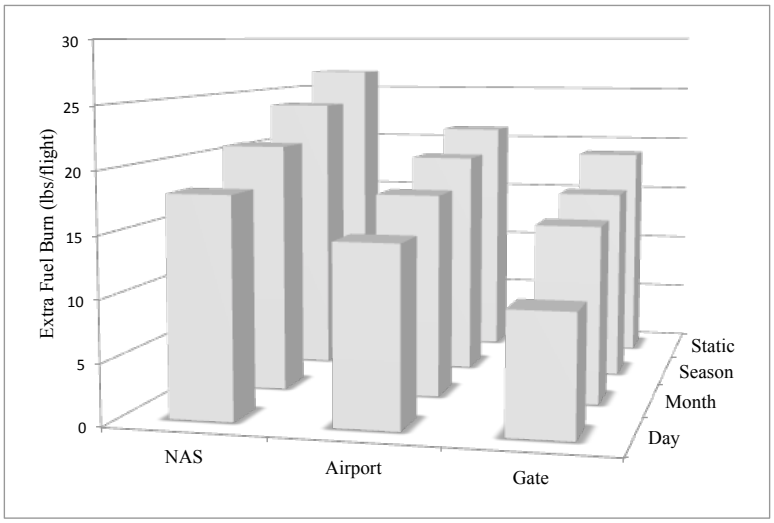

Figure 26. Estimates of the extra fuel burn for NAS adaptation types.

month adaptation has slightly less extra fuel burn than the Airport-Static adaptation. This suggests that publishing an FPA per month for the NAS may result in more fuel benefits than

publishing a year-round FPA for each major airport. The finest Gate-Day adaptation has an extra fuel burn of 10 lbs and recovers about 73% of the extra fuel burn of the NAS-Static adaptation.

VIII. Discussion

The motivation for a standard descent procedure for arriving small jet flights in the transition airspace is to improve trajectory predictability, especially near the top-of-descent region. The improved trajectory predictability leads to better airspace throughput and safety, which benefits not just the small jets but all flights. While Min-Fuel FPA provided the best fuel benefits, it is difficult to implement without datalink. Instead, two simpler strategies, Universal FPA and Descent-Speed FPA, were adapted to time, airspace, and direction to improve their fuel efficiency. The results showed that adaptation to gates and days could recover 50% to 70% of the extra fuel burn of the Airport-Static adaptation. Since regional jet operators consider fuel savings to the order of 10 lbs, the fuel-burn difference of 7 to 17 lbs per flight between the adaptation types may be important. Moreover, adaptation to shorter timespans may yield more fuel benefits in operation than estimated in the analysis, because high-fidelity weather data are unavailable for long look-ahead times such as a year, a season, or even a month. Variation of the performance envelope between aircraft, not modeled in the analysis, could compound with wind variation and raise the extra fuel burn, too. On the other hand, the speed brake usage, SB0, could be relaxed to reduce the extra fuel burn if it is determined that a certain level of relaxation would still maintain the required robustness of the procedure.

Looking towards the operational implementation of continuous descents under metering conditions, the FAA will have to decide upon an approach for defining continuous descent FPAs for small jets. While this paper compares and contrasts the relative fuel efficiency of candidate strategies for defining descent FPAs, other factors will enter the implementation decision, not the least of which will be the complexity and cost of implementing and supporting a fixed-FPA procedure. Universal FPA has the advantage of defining a single descent FPA for an airport. Descent-Speed FPA, while slightly more complex in terms of defining FPA as a function of descent speed, has the potential to capture much of the fuel efficiency related to the descent speed. Both strategies lend themselves to fast-time analysis that can support the selection and publication of their parameters a day or more before flight. This would allow the FAA to adapt the appropriate parameters to each airport and disseminate those parameters through the aeronautical information network. Depending on the time horizon chosen for the adaptation (annual, seasonal, monthly, weekly or daily), this information may be made available in several ways. For longer periods of time, the parame-

ters could be included as part of published arrival procedures or flight manual amendments. Alternatively, this information could be provided to pilots as part of their standard pre-flight planning and weather briefing. At the very least, this dissemination approach would be necessary for adaptations performed on a more frequent (e.g., daily) basis.

Given the sensitivity of the selected FPA to prevailing winds and the lack of a precise wind forecast for longer time horizons, analysis based on historical data or climatological data would lend itself to parameter adaptation on an annual, seasonal or monthly basis. Historical data from previous years may be used for such prediction, assuming a similar pattern of weather and wind. For shorter adaptation horizons, on the order of daily updates, numerical weather prediction such as the National Oceanic and Atmospheric Administration's Rapid Refresh weather forecast[34] (succeeding RUC) would provide precise and relatively accurate forecasts.

IX. Conclusion

Prediction of small jet descents has been challenging, as descent planning varies greatly from flight to flight and airline to airline. Lack of trajectory predictability makes it difficult for ATC to achieve Continuous Descent Arrivals (CDA) for these jets. This paper proposed a standard fixed-flight-path angle descent procedure for arriving small jets in the transition airspace in order to improve trajectory predictability and enhance airspace throughput. This standard descent procedure would help ground automation tools such as the Efficient Descent Advisor in delivering aircraft to the metering fix on time while maintaining separation.

Three strategies for choosing the descent FPA were presented. While the three strategies vary in operational complexity, they are expected to achieve the same level of trajectory predictability. The selection of the FPA considered fuel burn and flyability, which was modeled by the planned speed-brake usage. Adaptation to time, airspace, and direction was proposed to improve the fuel benefits of the two simple strategies: Universal FPA and Descent-Speed FPA. The Min-Fuel FPA strategy served as a reference point for the fuel-burn metrics. Analysis of the winds aloft at twelve major US airports led to the selection of the JFK, DFW, and LAX airports for the application of the FPA selection methodology. The three airports had very different degrees of wind variation and disparate arrival traffic flows. Results showed that the selection methodology successfully selected fuel-efficient and flyable FPAs for all three strategies, and the selected FPA correlated strongly with winds along the route. The Airport-Static adaptation of the Universal FPA burned by 14 to 26 lbs extra fuel per flight compared to the Min-Fuel FPA solution. The finest adaptation could potentially recover 50% to 70% of the extra fuel. Various factors affecting the fuel benefits of the simple strategies were investigated. Planned speed brake usage, when allowed in descent, would

decrease the extra fuel burn noticeably.

The fuel burn comparison in this work provides information for the design of a standard descent procedure in the transition airspace to support the CDA. Although the comparison focused on small jets, the analysis could apply to any jets that perform fixed-FPA descents. The choice of an economically appropriate adaptation type of the simple strategies can be NAS-wide, airport-specific, or gate-specific. It is ultimately incumbent on the the FAA to perform the cost-benefit analysis of potential implementations.

Appendix

The results of the three strategies applied to JFK and LAX that are not shown in Section VII are shown here for completeness.

Figure A.1: distributions of the FPAs selected by Min-Fuel FPA for JFK.

Figure A.2: γ_{univ} selected by the airport-specific adaptations of Universal FPA to JFK.

Figure A.3: γ_0 selected by the airport-specific adaptations of Descent-Speed FPA to JFK.

Figure A.4: values of γ_0 selected by the gate specific adaptations of Descent-Speed FPA to JFK.

Figure A.5: distributions of the FPAs selected by Min-Fuel FPA for LAX.

Figure A.6: γ_{univ} selected by the airport-specific adaptations of Universal FPA to LAX.

Figure A.7: γ_0 selected by the airport-specific adaptations of Descent-Speed FPA to LAX.

Figure A.8: γ_0 selected by the gate-specific adaptations of Descent-Speed FPA to LAX.

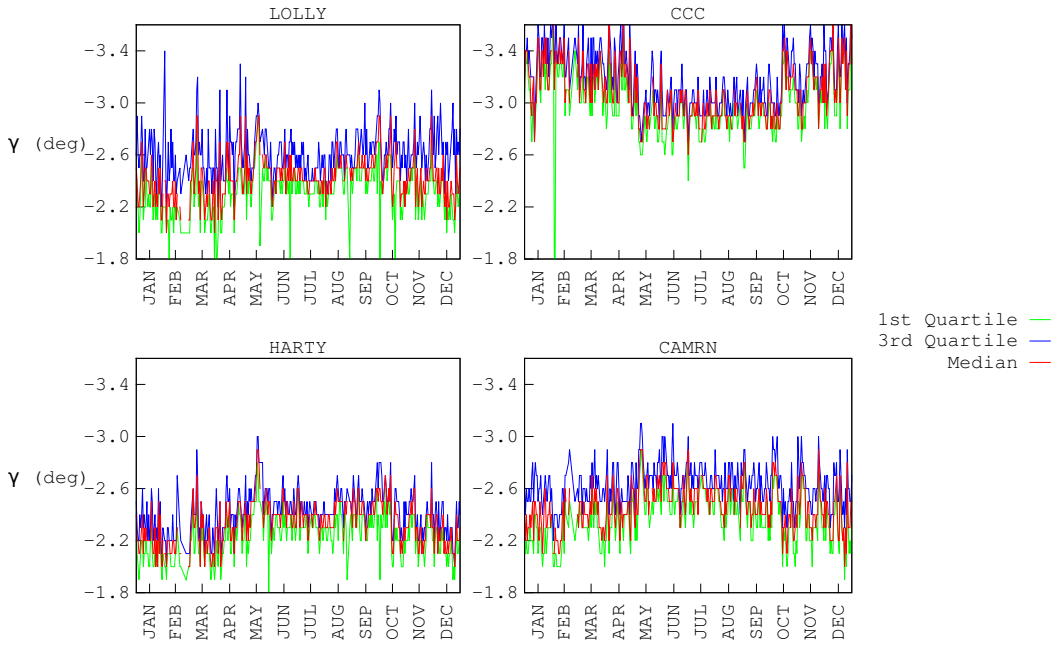

Figure A.1. The first quartile, third quartile, and median FPAs selected by Min-Fuel FPA for JFK.

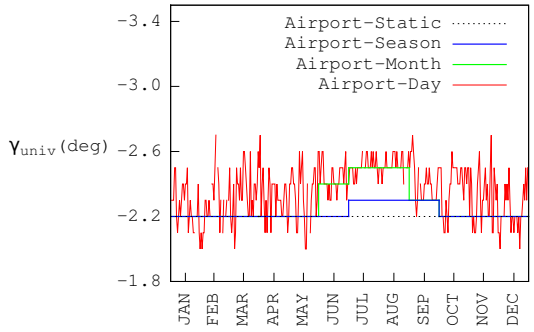

Figure A.2. Values of $\gamma_{\mathbf{univ}}$ selected for the airport-specific adaptations of Universal FPA to JFK.

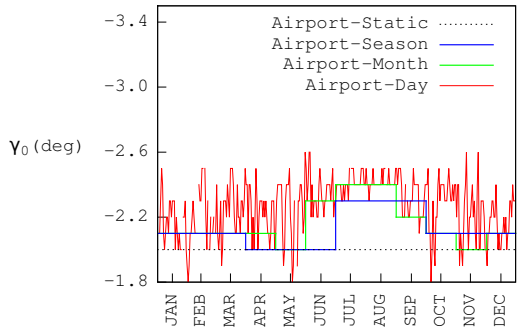

Figure A.3. Values of γ_0 selected by the airport-specific adaptations of Descent-Speed FPA to JFK.

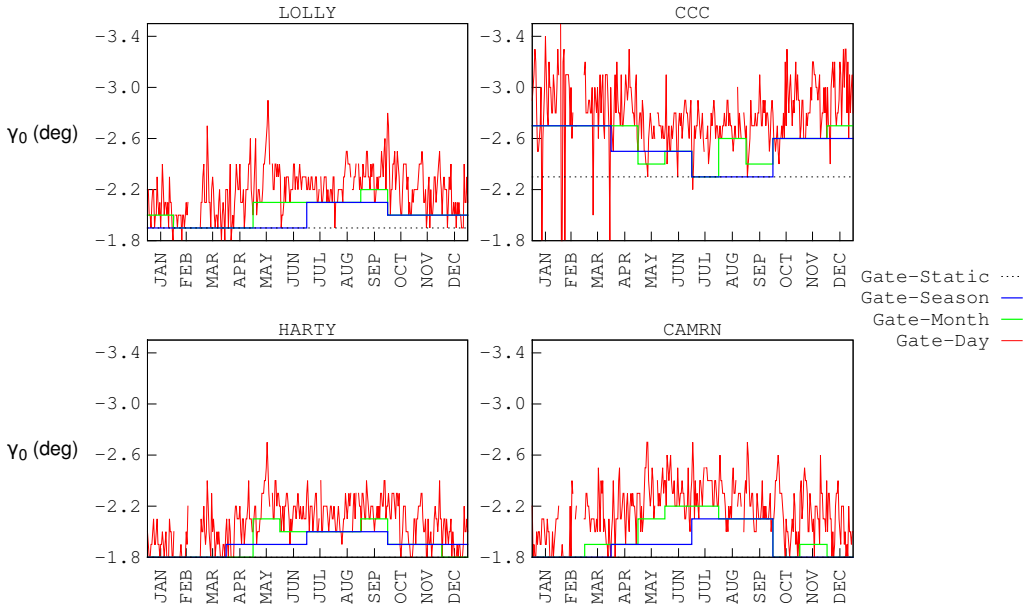

Figure A.4. Values of γ_0 selected by the gate-specific adaptations of Descent-Speed FPA to JFK.

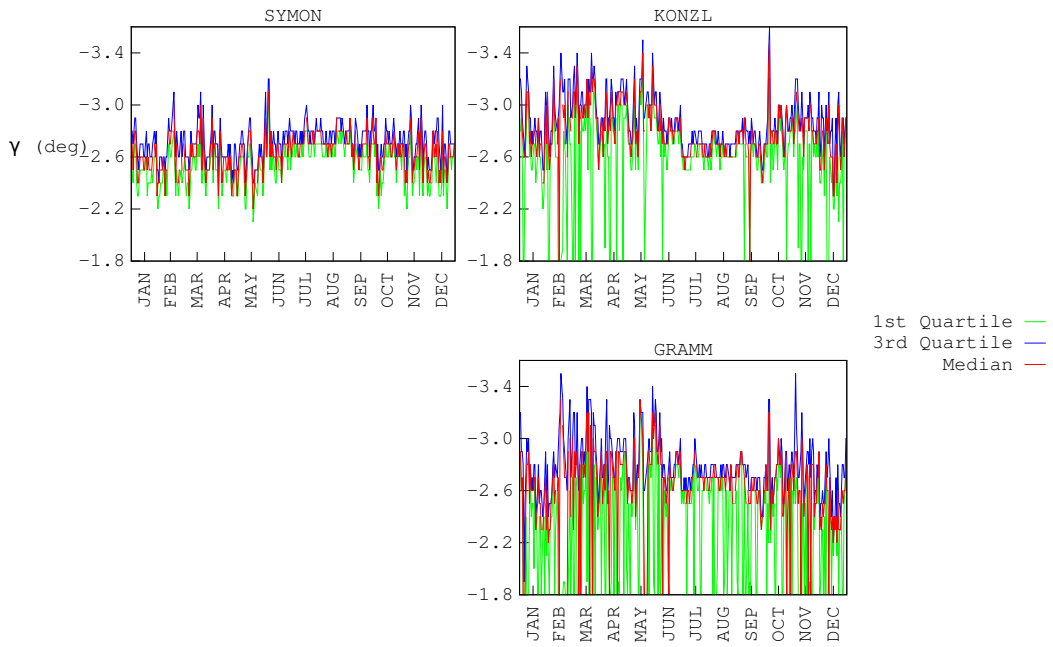

Figure A.5. The first quartile, third quartile, and median FPAs selected by Min-Fuel FPA for LAX.

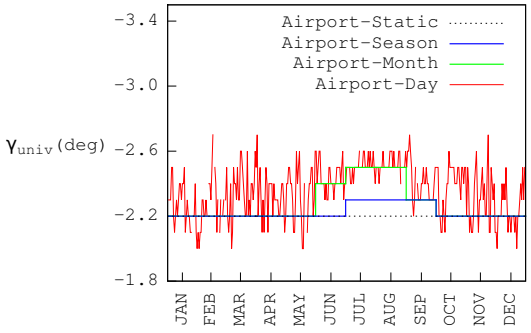

Figure A.6. Values of γ_{univ} selected by the airport-specific adaptations of Universal FPA to LAX.

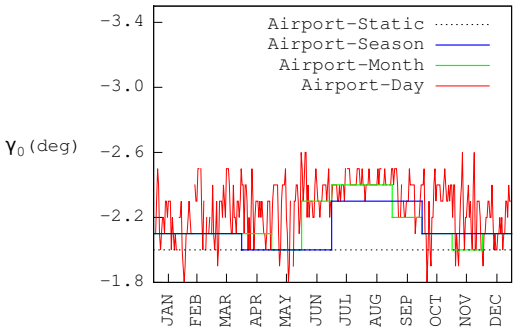

Figure A.7. Values of γ_0 selected by the airport-specific adaptations of Descent-Speed FPA to LAX.

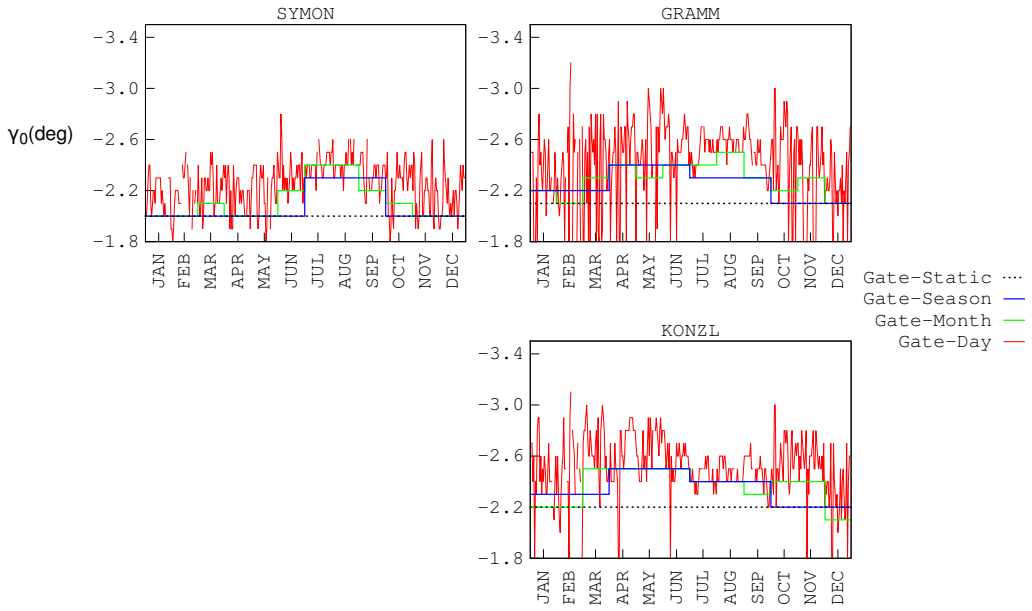

Figure A.8. Values of γ_0 selected for the gate-specific adaptations of Descent-Speed FPA to LAX.

References

[1]Coppenbarger, R. A., Nagle, G., Sweet, D., and Hayashi, M., "The Efficient Descent Advisor: Technology Validation and Transition," *Proceedings of the AIAA Aircraft Technology, Integration, and Operations Conference*, AIAA-2012-5611, Sept. 2012.

[2]"FAA's NextGen Implementation Plan," *Federal Aviation Administration*, March 2011.

[3]"Concept of Operations for the Next Generation Air Transportation System," *Joint Planning and Development Office (JPDO)*, Oct. 2009.

[4]Clarke, J.-P., Brooks, J., Nagle, G., Scacchioli, A., White, W., and Liu, S., "Optimized Profile Descent Arrivals at Los Angeles International Airport," *Journal of Aircraft*, Vol. 50, No. 2, 2013, pp. 360–369.

[5]Coppenbarger, R. A., Mead, R. W., and Sweet, D. N., "Field Evaluation of the Tailored Arrivals Concept for Datalink-Enabled Continuous Descent Approach," *Journal of Aircraft*, Vol. 46, No. 4, July-August 2009, pp. 1200–1209.

[6]Novak, D., Bucak, T., and Radišić, T., "Development, Design and Flight Test Evaluation of Continuous Descent Approach Procedure in FIR Zagreb," *PROMET - Traffic & Transportation*, Vol. 21, No. 5, Sept. 2009, pp. 319–329.

[7]Clarke, J.-P. B., Ho, N. T., Ren, L., Brown, J. A., Elmer, K. R., Tong, K.-O., and Wat, J. K., "Continuous Descent Approach: Design and Flight Test for Louisville International Airport," *Journal of Aircraft*, Vol. 41, No. 5, 2004, pp. 1054–1066.

[8]Robinson, J. E. and Kamgarpour, M., "Benefits of Continuous Descent Operations in High-Density Terminal Airspace Under Scheduling Constraints," *Proceedings of the 10th AIAA Aviation Technology, Integration, and Operations Conference*, AIAA-2010-9115, Sept. 2010.

[9]"FAA Aerospace Forecast Fiscal Years 2012-2032," *Federal Aviation Administration*, 2011.

[10]Swenson, H. N., Hoang, T., Engelland, S., Vincent, D., Sanders, T., Sanford, B., and Heere, K., "Design and Operational Evaluation of the Traffic Management Advisor at the Fort Worth Air Route Traffic Control Center," *Proceedings of the 1st USA/Europe Air Traffic Management R&D Seminar*, June 1997.

[11]Wu, M. G. and Green, S. M., "Analysis of Fixed Flight Path Angle Descents for the Efficient Descent Advisor," NASA/TM-2011-215992, Nov. 2011.

[12]Slater, G., "Study on variations in vertical profile for CDA descents," *Proceedings of the AIAA Aircraft Technology, Integration, and Operations Conference*, AIAA-2009-6912, Sept. 2009.

[13]Tong, K.-O., Schoemig, E., Boyle, D., Scharl, J., and Haraldsdottir, A., "Descent Profile Options for Continuous Descent Arrival Procedures within 3d Path Concept," *Proceedings of the IEEE/AIAA 26th Digital Avionics Systems Conference*, Oct. 2007, pp. 3.A.3–1 – 3.A.3–11.

[14]Izumi, K. H., "Sensitivity Studies of 4D Descent Strategies in an Advanced Metering Environment," *Proceedings of the American Control Conference, 1986*, June 1986, pp. 687–692.

[15]Izumi, K. H., Schwab, R. W., Groce, J. L., and Coote, A., "An Evaluation of Descent Strategies for TNAV-Equipped Aircraft in an Advanced Metering Environment ATOPS," Tech. Rep. NASA CR-178093, Boeing Commercial Airplane Company, Dec. 1986.

[16]Chakravarty, A., "Four-Dimensional Fuel-Optimal Guidance in the Presence of Winds," *Proceedings of the AIAA Guidance and Control Conference*, AIAA-1983-2242, Gatlinburg, Tenn., 1983.

[17]Lauderdale, T. A., Cone, A. C., and Bowe, A. R., "Relative Significance of Trajectory Prediction Errors on an Automated Separation Assurance Algorithm," *Proceedings of the 9th USA/Europe Air Traffic Management R&D Seminar*, June 2011.

[18]Stell, L., "Prediction of Top of Descent Location for Idle-thrust Descents," *Proceedings of the 9th USA/Europe Air Traffic Management R&D Seminar*, June 2011.

[19]Johnson, C., "Analysis of Top of Descent (TOD) uncertainty," *Digital Avionics Systems Conference (DASC), 2011 IEEE/AIAA 30th*, IEEE, 2011, pp. 2E3–1.

[20]Landry, S., Farley, T., Foster, J., Green, S., Hoang, T., and Wong, G. L., "Distributed Scheduling Architecture for Multi-Center Time-Based Metering," *Proceedings of the AIAA Aviation Technology, Integration, and Operations Conference*, AIAA-2003-6758, Nov. 2003.

[21]Nagle, G., Sweet, D., Carr, G., Felipe, V., Trapani, A., Coppenbarger, R., and Hayashi, M., "Human-in-the-Loop Simulation of the Efficient Descent Advisor for 3D Path Arrival Management," *Proceedings of the AIAA Aircraft Technology, Integration, and Operations Conference*, AIAA-2011-6877, Virginia Beach, VA, 2011.

[22]Coppenbarger, R., Dyer, G., Hayashi, M., Lanier, R., Stell, L., and Sweet, D., "Development and Testing of Automation for Efficient Arrivals in Constrained Airspace," *Proceedings of the 27th International Congress of the Aeronautical Sciences*, ICAS2010-11.11.3, Nice, France, 2010.

[23]Coppenbarger, R. A., Lanier, R., Sweet, D., and Dorsky, S., "Design and Development of the En Route Descent Advisor (EDA) for Conflict-Free Arrival Metering," *Proceedings of the AIAA Guidance, Navigation, and Control Conference*, AIAA-2004-4875, Aug. 2004.

[24]Mueller, K. T., Schleicher, D. R., and Coppenbarger, R. A., "Improved Aircraft Path Stretch Algorithms for the En Route Descent Advisor (EDA)," *Proceedings of the AIAA Guidance, Navigation, and Control Conference*, AIAA-2003-5571, Aug. 2003.

[25]Green, S. M. and Vivona, R. A., "En Route Descent Advisor Concept for Arrival Metering," *Proceedings of the AIAA Guidance, Navigation, and Control Conference*, AIAA-2001-4114, Aug. 2001.

[26]Henderson, J., Vivona, R. A., and Green, S. M., "Trajectory Prediction Accuracy and Error Sources for Regional Jet Descents," *Proceedings of the AIAA Guidance, Navigation, and Control Conference*, AIAA-2013-4535, 2013.

[27]Stell, L., "Analysis of Flight Management System Predictions of Idle-thrust Descents," *Proceedings of the IEEE/AIAA 29th Digital Avionics Systems Conference*, Oct. 2010.

[28]Sopjes, R., De Jong, P., Borst, C., Van Paassen, M., and Mulder, M., "Continuous Descent Approaches with Variable Flight-Path Angles under Time Constraints," *Proceedings of the AIAA Guidance, Navigation, and Control Conference*, AIAA-2011-6219, Aug. 2011.

[29]Benjamin, S. G., Brown, J. M., Brundage, K. J., Schwartz, B., Smirnova, T., Smith, T. L., Morone, L. L., and Dimego, G., "The Operational RUC-2. Preprints," *Proceedings of the 16th Conference on Weather Analysis and Forecasting*, Amer. Meteor. Soc., 1998, pp. 249–252.

[30]Lee, A. G., Bouyssounouse, X., and Murphy, J. R., "The Trajectory Synthesizer Generalized Profile Interface," *Proceedings of the 10th AIAA Aviation Technology, Integration, and Operations Conference*, AIAA-2010-9138, Sept. 2010.

[31]Slattery, R. and Zhao, Y., "Trajectory Synthesis for Air Traffic Automation," *Journal of Guidance, Control and Dynamics*, Vol. 20, No. 2, March 1997, pp. 232–238.

[32]Erzberger, H., Davis, T. J., and Green, S. M., "Design of Center-TRACON Automation System," *Machine Intelligence in Air Traffic Management, Andre Benoit, ed., AGARD CP-538*, Oct. 1993, pp. 11–1–11–12.

[33]Nuic, A., Poinsot, C., Iagaru, M.-G., Gallo, E., Navarro, F. A., and Querejeta, C., "Advanced Aircraft

Performance Modeling for ATM: Enhancements to the BADA Model," *Proceedings of the IEEE/AIAA 24th Digital Avionics Systems Conference*, Nov. 2005.

[34]Benjamin, S. G., Devenyi, D., Weygandt, T. S. S. S., Brown, J. M., Peckham, S., Brundage, K. J., Smith, T. L., Grell, G. A., and Schlatter, T. W., "From THE 13-KM RUC To the Rapid Refresh," *12th Conference on Aviation Range and Aerospace Meteorology*, 2006, pp. 9.1.1–9.1.4.